Author Manuscript

Author Manuscript

Author Manuscript

Author Manuscript

HHS Public Access

Author manuscript

Insect Biochem Mol Biol. Author manuscript; available in PMC 2021 May 01.

Published in final edited form as:

Insect Biochem Mol Biol. 2020 May ; 120: 103360. doi:10.1016/j.ibmb.2020.103360.

Heterogeneous Expression of the Ammonium Transporter *AgAmt* in Chemosensory Appendages of the Malaria Vector, *Anopheles gambiae*

Zi Ye[a], **Feng Liu**[a,d], **Huahua Sun**[a,d], **Mackenzie Barker**[b], **R. Jason Pitts**[c], **Laurence J. Zwiebel**[a,*]

[a]Department of Biological Sciences, Vanderbilt University, Nashville, TN 37235, USA

[b]Eastern Virginia Medical School, Norfolk, VA 23507, USA

[c]Department of Biology, Baylor University, Waco, TX 76706, USA

[d]These authors contributed equally to this study

Abstract

Ammonia is one of the principal kairomones originating from human and other animal emanations and in that context, plays an essential role in the host-seeking behaviors of the malaria vector mosquito *Anopheles gambiae*. Nevertheless, despite its importance in directing host-seeking, the mechanisms underlying ammonia detection in the mosquito olfactory system remains largely unknown. In addition to ongoing efforts to identify and characterize the molecular receptors that underlie ammonia sensitivity, previous studies have revealed a prominent role for ammonium transporters (Amt) in modulating antennal and behavioral responses in *Drosophila melanogaster* and *An. gambiae*. In the former, localization of *DmAmt* in antennal sensilla to auxiliary cells surrounding the ammonia sensory neurons led to the hypothesis that its role was to clear excess ammonium ions in the sensillar lymph. In the latter, RT-PCR and heterologous expression have been used to examine the expression and functional characteristics of the *An. gambiae* ammonium transporter, *AgAmt*. We now employ advanced transgenic tools to comprehensively examine *AgAmt* spatial localization across the peripheral chemosensory appendages in larvae and adult female *An. gambiae*. In the larval antennae, *AgAmt* appears localized in both neuronal and auxiliary cells. In contrast to *D. melanogaster*, in the adult antennae, *AgAmt*-derived signals are observed in both non-neuronal auxiliary cells and in sensory neurons in ammonia-responsive basiconic and coeloconic sensilla. In the maxillary palps, labella, and tarsi, *AgAmt* appears restricted to sensory neurons. We have also characterized the responses to ammonia of adult antennal coeloconic sensilla and maxillary palp capitate pegs revealing a correlation between sensillar *AgAmt* expression and ammonia sensitivity. Taken together, these data suggest that

*Corresponding author. Department of Biological Sciences, Vanderbilt University, Nashville, TN 37235, USA. l.zwiebel@vanderbilt.edu.

Publisher's Disclaimer: This is a PDF file of an unedited manuscript that has been accepted for publication. As a service to our customers we are providing this early version of the manuscript. The manuscript will undergo copyediting, typesetting, and review of the resulting proof before it is published in its final form. Please note that during the production process errors may be discovered which could affect the content, and all legal disclaimers that apply to the journal pertain.

Author Manuscript Author Manuscript Author Manuscript Author Manuscript

AgAmt may play heterogeneous roles in the adult and larval chemosensory apparatus and potentially broad utility as a supra-receptor target in mosquito control.

Keywords

Anopheles gambiae ammonium transporter; chemosensory system; cellular organization; Q system; phiC31 integration

1. Introduction

Mosquito vectors are responsible for the transmission of a variety of deadly human diseases, including dengue fever, yellow fever, Zika virus, West Nile virus, lymphatic filariasis, and malaria (Van Der Goes Van Naters and Carlson, 2006). In 2016, more than 200 million cases of human malaria occurred worldwide (Alonso and Noor, 2017). The malaria mosquito *Anopheles gambiae* is one of the primary vectors of the most prevalent malaria parasite *Plasmodium falciparum* (Molina-Cruz et al., 2016; Report, 1980). Female mosquitoes ingest blood meals that are required for egg development and through which the parasite is vectored by *Anopheles* mosquitoes and is transmitted from human to human (Cox, 2010). Mosquitoes rely on their acute olfactory system to detect volatiles, including CO_2, ammonia, and other specific odors to locate humans and other mammals which represent potential blood meal hosts (VanDer Goes Van Naters and Carlson, 2006; Zwiebel and Takken, 2004).

In mosquitoes, the primary head appendages involved in odorant detection are the antennae, maxillary palps, and the labella of the proboscis. Dispersed along the surface of those appendages are hollow sensory hairs known as sensilla. A large variety of olfactory sensory neurons (OSNs) are housed in the sensilla and respond to distinct spectrums of odorants (Guidobaldi et al., 2014; Montell and Zwiebel, 2016). Based on the morphological features, olfactory sensilla are categorized as trichoid, basiconic (also known as grooved pegs), and coeloconic (Pitts and Zwiebel, 2006). Although different functional subgroups are present within these classes of sensilla, grooved pegs are generally tuned to acids and amines, trichoid sensilla respond to a broader spectrum of odors (Qiu et al., 2006), while coeloconic sensilla have been associated with both chemo- and thermosensory pathways (McIver, 1973). Within chemosensory sensilla, OSNs are positioned in an aqueous lymph that fills the luminal space and contains odorant binding proteins (OBPs) and odorant-degrading enzymes (ODEs) and other components that are required for odorant recognition and clearage (Leal, 2013). On OSN dendritic membranes, several families of ligand-gated ion channels including odorant receptors (ORs), gustatory receptors (GRs) and ionotropic receptors (IRs), play central roles in olfactory signal transduction as they are activated by specific odorants to generate the action potentials representing peripheral odor coding (Suh et al., 2014).

Ammonia is a volatile component of mammalian sweat and electrophysiological studies have revealed a broad set of neuronal responses to ammonia in antennal trichoid sensilla and grooved pegs (Meijerink et al., 2001; Qiu et al., 2006). As a component of a hyper-effective five-compound mosquito blend, ammonia has been shown to attract female *An. gambiae* (Boverhof et al., 2008; Mukabana et al., 2012; Smallegange et al., 2005, 2002). While

Author Manuscript Author Manuscript Author Manuscript Author Manuscript

studies in *D. melanogaster* have suggested DmIr92a is a functional ammonia receptor, little is known about the molecular and indeed the neuronal receptors responsible for ammonia detection in mosquitoes (Benton et al., 2009; Min et al., 2013), especially as no clear homologs of DmIr92a are encoded in mosquito genomes.

Nitrogen is essential for the survival of mosquitoes and indeed all living organisms and ammonium is the principal ionic target for its fixation and subsequent incorporation into biological molecules. At the same time, ammonia is toxic when it accumulates, which makes it critical for cells to have efficient mechanisms for the uptake and transport of ammonium (Bittsánszky et al., 2015; Crawford and Forde, 2002). Because ammonium is not able to penetrate the cell membrane passively, ammonium transport proteins, including ammonium transporters (Amts), methylammonium/ammonium permeases (Meps), and Rhesus (Rh) proteins, facilitate the cross-membrane transportation of ammonium (Andrade and Einsle, 2007). Recently, several groups have reported the characterization of antennal-expressed Amt proteinsin both *Drosophila* and *Anopheles* (Menuz et al., 2014; Pitts et al., 2014).

In *D. melanogaster, DmAmt* has been shown to be directly involved in ammonia detection as null mutants show significantly reduced olfactory responses to ammonia than the wild type (Menuz et al., 2014). Localization of *DmAmt* in the fruit fly antennae revealed that it is expressed in the auxiliary cells surrounding ammonia sensitive neurons, suggesting that DmAmt is not the receptor/sensor but rather is involved in ammonium clearance from the sensillar lymph (Menuz et al., 2014). This finding suggests that DmAmt's role is to prevent DmIr92a from being prematurely desensitized by the accumulation of environmental (sensory) ammonia or ammonia otherwise produced by cellular metabolism (Menuz et al., 2014; Trussell and Fischbach, 1989).

In *Aedes aegypti*, the reduced expression of *AeAmt1* caused accumulation of ammonium in the mosquito larval hemolymph which suggested its role in ammonium excretion (Chasiotis et al., 2016). In *An. gambiae*, while the functional role of AgAmt in mediating antennal ammonia sensitivity remains unclear, its transcripts are highly abundant in female antennae and have been functionally shown to modulate ammonium cross-membrane transportation using *Xenopus* heterogeneous expression system (Pitts et al., 2014). In addition, *AgAmt* was shown to phenotypically rescue the defect of ammonia responses in *DmAmt* mutants (Menuz et al., 2014).

In order to better understand the role of *AgAmt* in ammonia detection in *An. gambiae*, we now have characterized its tissue and cellular localization utilizing several advanced transgenic tools, including the newly developed "Q system" (Potter et al., 2010). The comprehensive cellular localization of *AgAmt* in the chemosensory system of larval and adult-stage *An. gambiae* informs our understanding of the role of this transporter in host-seeking and other important behaviors.

Author Manuscript Author Manuscript Author Manuscript Author Manuscript

2. Material and Methods

2.1 Mosquito maintenance

An. gambiae phiC31 docking line E was acquired from The Malaria Research and Reference Reagent Resource Center (Meredith et al., 2011). *An. gambiae* effector line (*QUAS-mCD8:GFP*) was a generous gift from the lab of Dr. C. Potter at The Johns Hopkins University School of Medicine (Riabinina et al., 2016). All the mosquito lines were reared at 27°C, 75% relative humidity under a 12:12 light-dark cycle and supplied with 10% sugar water in the Vanderbilt University Insectary.

2.2 *AgAmt promoter-QF2* construct

The 1kb/3kb *AgAmt* upstream sequence was amplified from the wild type *An. gambiae* genomic DNA using the forward primers (AgAmt_1kb_F: 5'- AAT CCG GAA CAA GCA TCA TCA GAG CGA T −3'; AgAmt_3kb_F: 5'- AAT CCG GAC CCA AGT AAT TAA GTA GTG CT −3') and the reverse primer AgAmt _R (5'- AAG GCG CGC CTG CAG TGC TAA TCA AAC CAA C −3'). The 1kb/3kb *AgAmt promoter* (*AgAmtP*) amplicons were restriction enzyme digested and inserted into the BspEI/AscI restriction site on a pBattB-DsRed construct (Supplementary data). Likewise, the *QF2* sequence was sequentially amplified from the pXL-BACII-DsRed-QF2-hsp70 construct (Riabinina et al., 2016) using the primer pair QF2for (5'- AAG GCC GGC CAT GCC ACC CAA GCG CAA AAC- 3') and QF2rev (5'- AAG CGA TCG CTC ACT GTT CGT ATG TAT TAA TG- 3') and inserted into the FseI/AsiSi restriction site which is downstream of the *AgAmtP* insertion site.

2.3 Mosquito transgenics

The detailed microinjection protocol was described previously (Pondeville et al., 2014). Briefly, newly laid (approximately 1hr-old) embryos of the phiC31 docking line (Meredith et al., 2011) were immediately collected and aligned on a filter paper moistened with 25mM sodium chloride solution. All the embryos were fixed on a coverslip with double-sided tape and a drop of halocarbon oil 27 was applied to cover the embryos. The coverslip was further fixed on a slide under a Zeiss Axiovert 35 microscope with a 40X objective. The microinjection was performed using Eppendorf FemtoJet 5247 and quartz needles (Sutter Instrument, Novato, CA). The phiC31 integrase was provided by the pENTR R4-vas2-integrase-R3 helper plasmid (a kind gift from Eric Marois via Addgene plasmid #62299) which was diluted to 200ng/μl in 1x microinjection buffer (5mM KCl, 0.1mM sodium phosphate buffer, pH7.2) before being co-injected with the pBattB-DsRed-AgAmtP-QF2 plasmid at 400ng/μl. The injected embryos were placed into deionized water with artificial sea salt (0.3g/L) and reared in the lab condition.

First generation (G_0) of injected adults were separated based on gender and crossed to 5X phiC31 docking line gender counterparts. Their offspring (F_1) was screened for DsRed-derived red eye fluorescence. Red-eyed F_1 males were individually crossed to 5X docking line females to establish a stable transgenic line. PCR analysesof all individuals were performed (after mating) to validate phiC31 integration using the primer pairs attR_F (5'- TCA AAC TAA GGC GGA GTG G −3') and attR_R (5'- GAT GGG TGA GGT GGA GTA

Author Manuscript Author Manuscript Author Manuscript Author Manuscript

CG −3'); attL_F (5'- GAG GTC GAC GAT GTA GGT CAC −3') and attL_R (5'- ACC TTT TCT CCC TTG CTA CTG AC −3') that covers the junctions between the integrated and endogenous sequences (Meredith et al., 2011). The presence of *1kb/3kb AgAmtP-QF2* sequences was PCR validated using primers 1kb_F (5'- GCC ATC CAA CTC ACC ACA CA −3'), 3kb_F (5'- CGG CAA AAG AAG GGT TTC GG −3'), and QF_R (5'- CAG GGT CGT AGT TGT GGG TC −3').

2.4 Whole-mount appendage imaging

Because the driver line was not homozygous, all the offspring from the cross between the *AgAmtP-QF2* driver line and the *QUAS-mCD8:GFP* effector line (Riabinina et al., 2016) were collected and screened for the presence of DsRed in the eye. Whole antennae from adult females and larvae were thereafter dissected into 4% formaldehyde in PBST (0.1% Triton X-100 in PBS) and fixed on ice for 30mins. Samples were washed 3X in PBST for 10mins each and transferred onto slides and mounted in Vectashield fluorescent medium (Vector Laboratories, Burlingame, CA).

2.5 Immunocytochemistry

Antibody staining was performed as previously (Pitts et al., 2004) with minor modifications. Antennae, labella, maxillary palps, and tarsi were dissected into 4% formaldehyde in PBST and fixed on ice for 30mins. Samples were wash 3X in PBST for 10mins each and then embedded in TFM Tissue Freezing Medium (General Data Company Inc., Cincinnati, OH). Cryosections were obtained at −20°C with a CM1900 cryostat (Leica Microsystems, Bannockburn, IL). Samples were sectioned at ~10μm and transferred onto Superfrost plus slides (VWR Scientific, Radnor, PA). Slides were air-dried at room temperature (RT) for 30mins and fixed in 4% formaldehyde in PBST for 10mins, followed by 3X rinsing in PBST for 10mins each. Thereafter, 5% normal goat serum (Sigma-Aldrich, St. Louis, MO) in PBST was applied and the slides were blocked in dark at RT for 1hr with HybriWell sealing chambers (Grace Bio-Labs, Bend, OR). Primary antibody (Rabbit α-Orco/Goat α-HRP-Cy3) was diluted 1:500 in 5% normal goat serum in PBST and applied on the slides and incubated overnight at 4°C. After primary antibody staining, slides were washed 3X in PBST for 10mins each and stained with secondary antibody Goat α-Rabbit-Cy3 (Jackson ImmunoResearch, West Grove, PA) 1:500 in 5% normal goat serum PBST for 2hrs at RT and then rinsed 3X. Nuclei were stained with 300nM DAPI (Invitrogen, Carlsbad, CA) at RT for 10mins. Slides were briefly washed and mounted in Vectashield fluorescent medium (Vector Laboratories, Burlingame, CA). α-HRP-Cy3 staining was directly visualized without the use of secondary antibody.

The whole-mount larval antennae were dissected into 4% formaldehyde in PBST and fixed on ice for 30mins. Samples were washed 3X in PBST for 10mins each and blocked with 5% normal goat serum (Sigma-Aldrich, St. Louis, MO) in PBST overnight at 4°C. Then 1:500 primary antibody (Rabbit α-Orco/Goat α-HRP-Cy3) was added and the samples were incubated overnight at 4°C. After primary antibody staining, samples were washed 3X in PBST for 10mins each and stained with secondary antibody Goat α-Rabbit-Cy3 (Jackson ImmunoResearch, West Grove, PA) 1:500 in 5% normal goat serum PBST overnight at 4°C and then rinsed 3X. Nuclei were stained with 300nM DAPI (Invitrogen, Carlsbad, CA) at

Author Manuscript Author Manuscript Author Manuscript Author Manuscript

4°C for 1hr. Samples were transferred onto the slides and mounted in Vectashield fluorescent medium (Vector Laboratories, Burlingame, CA). α-HRP-Cy3 staining was directly visualized without the use of secondary antibody.

2.6 Fluorescence In-situ hybridization (FISH)

The TOPO-TA dual promoter vector (Invitrogen, Carlsbad, CA) was used to subclone full length *AgIr76b* as described in the previous study (Pitts et al., 2017). Similarly, the full length *AgGr15* coding sequence was cloned into the TOPO-TA dual promoter vector and verified by DNA sequence analysis. Antisense/sense probes were thereafter synthesized using SP6/T7 RNA polymerase (NEB, Ipswich, MA) with Digoxigenin (DIG) RNA Labeling Kit (Roche, Switzerland).

Antennal samples were sectioned and fixed as described above. Sequentially, the slides were incubated in acetylation solution (0.1M triethanolamine, 0.65% HCl, 0.375% acetic anhydride) for 10mins at RT. After being washed 3X in PBST, slides were incubated in pre-heated (65°C) hybridization buffer (50% deionized formamide, 5X saline sodium citrate (SSC), 50μg/mL heparin sodium salt, 0.1% tween-20) for 40mins at RT. RNA probes were diluted in the hybridization buffer at 500ng/mL and applied onto the slides which were further incubated with sealing chambers at 65°C for 18hrs.

Following the hybridization, slides were washed 3X in 0.2X SSC at 65°C for 20mins each and then placed in TNT buffer (0.1M Tris-HCl, 150mM NaCl, 0.05%Tween-20) at RT for 10mins. TNB buffer (0.1M Tris-HCl, 150mM NaCl, 0.05%Tween-20, 1% blocking reagent from PerkinElmer) was subsequently applied to the slides for blocking for 1hr at RT inside sealed hybridization chambers. Due to the extreme overnight incubation temperature of FISH (65°C) that bleached the fluorescence of GFP, the GFP signal was recovered using GFP antibody (α-GFP) after the FISH experiment. Primary antibodies including 1:200 Chicken α-GFP (Vanderbilt Antibody and Protein Resource) and 1:500 Sheep α-DIG-POD (Roche, Switzerland) in TNB were applied to the slides which were thereafter incubated at 4°C overnight. After washing (3X) in TNT at RT for 5mins each, secondary antibody (1:1000 Donkey α-Chicken-Alexa488; Jackson ImmunoResearch, West Grove, PA) in 5% normal donkey serum TNT was applied to the slides which were incubated for 2hrs at RT. The slides were subsequently washed 3X in TNT at RT for 5mins each. TSA-Cy3 amplification (PerkinElmer, Waltham, MA) was performed according to the manufacturer's instructions at 1:50 in amplification working buffer at dark, following by 3X washing in TNT for 5mins each and mounting in Vectashield fluorescent medium (Vector Laboratories, Burlingame, CA).

2.7 Confocal microscopy

Confocal microscopy images at 1024*1024 pixel resolution were collected on an Olympus FV-1000 equipped with a 100X oil objective at the Vanderbilt University Cell Imaging Shared Resource Core. Lasers wavelengths of 405nm, 488nm, and 543nm were used to detect DAPI, GFP, and Cy3, respectively.

Author Manuscript Author Manuscript Author Manuscript Author Manuscript

2.8 Electrophysiology

Single sensillum recording (SSR) were carried out as previously described (Liu et al., 2013) with minor modifications. Mated female mosquitoes (4–10 days after eclosion) were mounted on a microscope slide (76 × 26 mm) (Ghaninia et al., 2007). The antennae were fixed using double-sided tape to a cover slip resting on a small bead of dental wax to facilitate manipulation and the cover slip was placed at approximately 30 degrees to the mosquito head. Once mounted, the specimen was placed under an Olympus BX51WI microscope and the antennae viewed at high magnification (1000×). Two tungsten microelectrodes were sharpened in 10% KNO2 at 10 V. The grounded reference electrode was inserted into the compound eye of the mosquito using a WPI micromanipulator and the recording electrode was connected to the preamplifier (10×, Syntech) and inserted into the shaft of the olfactory sensillum to complete the electrical circuit to extracellularly record OSN potentials (Den Otter et al., 1980). Controlled manipulation of the recording electrode was performed using a Burleigh micromanipulator (Model PCS6000). The preamplifier was connected to an analog to digital signal converter (IDAC-4, Syntech), which in turn was connected to a computer for signal recording and visualization.

Ammonium hydroxide (Sigma-Aldrich, St. Louis, MO) was serially diluted (in water) to 0.01%, 0.05%, 0.1%, 0.5%, 1%, and 5% ammonia solutions. For each concentration, a 10μl aliquot was applied onto a filter paper (3 × 10mm) which was then inserted into a Pasteur pipette to create the stimulus cartridge. A sample containing the solvent (water) alone served as the control. The airflow across the antennae was maintained at a constant 20 ml/s throughout the experiment. Purified and humidified air was delivered to the preparation through a glass tube (10-mm inner diameter) perforated by a small hole 10cm away from the end of the tube into which the tip of the Pasteur pipette could be inserted. The stimulus was delivered to the sensilla by inserting the tip of the stimulus cartridge into this hole and diverting a portion of the air stream (0.5L/min) to flow through the stimulus cartridge for 500ms using a stimulus controller (Syntech). The distance between the end of the glass tube and the antennae was ⩽1cm. Signals were recorded for 10s starting 1 second before stimulation, and the action potentials were counted off-line over a 500ms period before and after stimulation. Spike rates observed during the 500ms stimulation were subtracted from the spontaneous activities observed in the preceding 500ms and counts recorded in units of spikes/s.

3. Results

3.1 Generation of *AgAmtP-QF2* driver line

Significant efforts to directly localize AgAmt protein or *AgAmt*-derived transcripts proved unsuccessful due to the paucity of specific immunological reagents and riboprobes. To address this deficit, the “Q” binary expression system recently brought to *An. gambiae* (Riabinina et al., 2016) was utilized to indirectly visualize *AgAmt* expression. Here an *AgAmtP-QF2* driver line was generated and subsequently crossed to a *QUAS-mCD8:GFP* effector line to generate *AgAmtP-QF2, QUAS-mCD8:GFP* progeny lines. In this way, *AgAmtP* elements regulate the expression of *QF2* which in turn binds to *QUAS* elements to robustly drive the expression of visible *mCD8:GFP* markers to indirectly reveal the likely

Author Manuscript Author Manuscript Author Manuscript Author Manuscript

sites of *AgAmt* expression. Inasmuch as subsequent studies rely on these indirect binary markers, we acknowledge the inherent caveats of this system in our characterization of *AgAmt* expression.

To begin with we took advantage of the site-specific integration phiC31 system to generate a driver line by integrating the *AgAmtP-QF2* construct into a pre-defined genomic site (Meredith et al., 2011). Because of our imprecise understanding of the all the features of the *AgAmtP*, we initially chose to incorporate 1kb and 3kb upstream sequences from the *AgAmt* start codon as potential *AgAmt* regulatory sequences to generate two independent transgenic driver lines (1kb/3kb *AgAmtP-QF2* drivers). Microinjection of preblastoderm embryos was used to deliver the *AgAmtP-QF2* construct containing an *attB* attachment site and a *3xP3-DsRed* marker (pBattB-*DsRed*-1kb/3kb *AgAmtP-QF2*) along with a phiC31 integrase encoding helper plasmid regulated by the vasa2 promoter to induce the integration in germ cells (Table 1). Individual males with red fluorescence in the eye and ventral nerve cord fluorescence were crossed to docking line females to establish transgenic lines. The successful integration was confirmed using genomic DNA PCR to show amplicons that cover the junctions between the endogenous and integrated sequences (Figure 1A–1G).

3.2 Specific *AgAmt* localization driven by the “Q system”

We first examined whole-mount female antennal samples of both the 1kb/3kb

AgAmtP-GFP progeny where *AgAmtP*-driven expression was specific to the grooved pegs and coeloconic sensilla (1kb *AgAmtP-GFP*: Figure 2A, 2B; 3kb *AgAmtP-GFP*: Figure 2C, 2D). Importantly, except for the nonspecific expression inherent to the effector line (Riabinina et al., 2016), no *GFP* expression was observed in chemosensory appendages in either parental strain (Supplementary data; Figure S1).

While *AgAmtP*-driven *GFP* is expressed in all coeloconic sensilla, it was only observed in a subset of grooved pegs. In order to assess the relative *GFP* expression patterns of both these lines, the total number of GFP-labelled grooved pegs (Supplementary data; Table S1 & Figure S2A) and coeloconic sensilla (Supplementary data; Table S2 & Figure S2B) were counted and compared between the 1kb *AgAmtP-GFP* progeny and the 3kb *AgAmtP-GFP* progeny. These quantitative data suggest there is no significant difference between the percentage of GFP-labelled grooved pegs (Supplementary data; Table S3; p-value = 0.1061) in the 1kb (99.30% as the observed percentage in the statistical test) and 3kb (96.97% as the expected percentage in the statistical test) *AgAmtP-GFP* progeny. This suggests that the major regulatory elements that comprise the *AgAmtP* are likely to be contained within the region that is 1kb upstream from the start codon. However, inasmuch as this comparison was not based on cellular expression, we appreciate that there may still be subtle GFP signal expression/intensity differences between the two lines. Nevertheless, in the absence of significant expression differences, all studies were henceforth carried out using the 1kb *AgAmtP-GFP* progeny.

3.3 Heterogeneous *AgAmt* expression in olfactory appendages

We first investigated whether *AgAmt* is expressed in non-neuronal auxiliary cells where, as was observed for *DmAmt* (Menuz et al., 2014) it might function in clearing ammonium from

Author Manuscript Author Manuscript Author Manuscript Author Manuscript

the sensillar lymph. Neurons were labelled using a horseradish peroxidase antibody (α-HRP-Cy3), which has been previously used as a general neuronal marker in *Drosophila* and mosquitoes (Jan and Jan, 1982; Loesel et al., 2006; Pitts et al., 2004). An examination of female antennal cryosections revealed that *AgAmtP*-driven *GFP* is expressed in both neuronal and non-neuronal cells across multiple flagellomeres on antennae (Figure 3A–3D). Z-axis projections of whole-mount antennal images revealed both coeloconic sensilla and grooved pegs are innervated with likely *AgAmt*-expressing neurons (Figure 3E–3H). Here, we observed characteristically distinct cellular morphology between *AgAmtP*-driven GFP labelled neurons and auxiliary cells. While the likely *AgAmt*-expressing neuron cell bodies are typically circular, the shapes of the non-neuronal cells are more irregular, consistent with the expected morphology of thecogen, tormogen, and trichogen sensillar auxiliary cells (Mclver, 1982; Shanbhag et al., 2000). In some instances, a partial overlap between *AgAmt* and α-HRP labelling was observed, which might be due to cell stacking on the z-axis. This also supports a close association between potentially *AgAmt*-expressing auxiliary cells and sensory neurons (Figure 3I–3L).

Immunohistochemistry and fluorescence *in situ* hybridization (FISH) were used to further investigate the relationship between *AgAmt* and discrete sets of chemosensory receptors to discriminate subclasses of chemosensory neurons. In these studies, polyclonal antibodies to the Anopheline orthologs of the OR co-receptor (AgOrco) and riboprobes to the IR co-receptor (AgIr76b) allowed us to label antennal odorant receptor neurons (ORNs) (Pitts et al., 2004) and ionotropic receptor neurons (IRNs) independently (Pitts et al., 2017). We elected to focus on *AgIr76b* as its homolog in *Drosophila* is expressed in the same neurons as the ammonia receptor, *DmIr92a* (Benton et al., 2009). These studies revealed neither co-localization nor a close association between *AgAmt*- and *Orco*-expressing cells (Figure 4A–4D), while *AgIr76b* antisense riboprobes shows a close association between *Ir76b*-expressing IRNs and potentially *AgAmt*-expressing auxiliary cells (Figure 5A, 5B). Taken together, these data suggest that *AgAmt* is likely to be expressed in auxiliary cells surrounding *IR*-expressing IRNs. As a negative control, *AgIr76b* sense riboprobes failed to label any cells or structures other than the antennal cuticle (Figure 5C, 5D). Surprisingly, in contrast to the labelling studies of the antennae, *AgAmtP*-driven GFP signals were co-localized with a discrete subset of *Orco*-expressing ORNs in the female maxillary palps where only a very small portion of ORNs (approximately less than 5%) were likely to be *AgAmt*-positive (Figure 6A–6C).

3.4 Olfactory responses of capitate pegs and coeloconic sensilla to ammonia

The localization of *AgAmtP*-driven GFP in subpopulations of coeloconic sensilla on the antennae and maxillary palp capitate pegs begs the question as to ammonia response profiles of those structures. Single sensillum recordings (SSRs) were carried out to investigate dose-dependent responses of these sensilla to ammonia at 6 different concentrations (0.01%−5%), with a specific focus on the 5th-8th antennal flagellomeres where consistent *AgAmtP*-derived GFP expression in coeloconic sensilla was observed. SSR studies identified significant and dose-dependent ammonia responses in all tested antennal coeloconic sensilla (n=14) (Figure 7A, 7B). In maxillary palp capitate pegs, the cpB and cpC neurons typically display lower spike amplitudes than cpA neurons (Lu et al., 2007), and were therefore

Author Manuscript Author Manuscript Author Manuscript Author Manuscript

counted together due to the technical difficulty of separation. Dose-dependent excitatory responses to ammonia were identified in only cpB/C neurons; in contrast to either no response or slightly inhibitory responses displayed in cpA neurons (n=6) (Lu et al., 2007) (Figure 7C, 7D).

3.5 Neuronal *AgAmt* expression in gustatory appendages

While the labella and tarsi are considered to be the primary gustatory appendages of the mosquito, previous studies have revealed robust olfactory responses in the labial sensilla of *An. gambiae* (Kwon et al., 2006; Saveer et al., 2018). To investigate the potential role of *AgAmt* in these appendages, cryosections were examined using immunohistochemistry and FISH. To begin with, GFP-labelled cells were counted and compared in labella between the 1kb *AgAmtP-GFP* and the 3kb *AgAmtP-GFP* lines (Supplementary data; Table S4). Analysis using unpaired t-tests suggests there is no significant difference in the number of GFP-labelled cells between these lines (Supplementary data; Figure S3; p-value = 0.874). Z-axis projections of labellum whole-mounts showed intensive *AgAmtP*-driven *GFP* expression that was relatively uniform throughout the entire appendage where *AgAmtP*-derived *GFP* expressing neurons were found across the gustatory T1 sensilla (Figure 8A–8D) (Saveer et al., 2018), a pattern that is markedly different from the antennae. Furthermore, α-HRP-Cy3 (Figure 9A–9D), α-Orco immunostaining (Figure 9E–9H) and *AgIr76b* FISH (Figure 10), revealed that *AgAmtP*-derived *GFP* expression in the labellum is strictly neuronal, distributed across distinct populations of *AgOrco*-expressing ORNs and *AgIr76b*-expressing IRNs.

In the *D. melanogaster* labellum, *DmAmt* is not involved in volatile or contact-based ammonia sensing but instead is expressed in sugar sensing *Gr5a* neurons (Delventhal et al., 2017). To investigate whether *AgAmt* has a similar expression pattern, we used FISH to localize *AgGr15* which is the homolog to *DmGr5a*. In these studies, we found extensive co-localization between *AgAmtP*-driven GFP and *AgGr15* (Figure 11A–11D; negative control with *AgGr15* sense riboprobe: Figure 11E–11H). In the *An. gambiae* tarsi, *AgAmtP*-derived *GFP* expression was uniformly observed across all 5 tarsal segments of prothoracic, mesothoracic, and metathoracic tarsi where it co-localizes with α-HRP-Cy3, indicating once more that *AgAmtP*-derived *GFP* is expressed in neurons (Figure 12A–12C). These likely *AgAmt*-expressing cells are localized to the distal half of each tarsal segment in close proximity to the joints between segments where a cluster of neurons are localized.

3.6 Larval *AgAmt* expression

Larval progeny from both the 1kb and 3kb *AgAmtP-QF2* driver lines house a cluster of GFP + potentially *AgAmt*-expressing cells proximal to the sensory cone (Figure 13), which is the major olfactory structure on the multi-articulated larval antennae (Xia et al., 2008). Interestingly, significantly fewer cells were labelled in the 1kb *AgAmtP-GFP* progeny (Figure 13A) as compared to the 3kb progeny (Figure 13B), suggesting the presence of larval specific transcriptional control elements between 1kb and 3kb upstream of the *AgAmt* translational start site. As such, sequential experiments were conducted using the 3kb *AgAmtP-GFP* progeny. Consistent with the adult female antennae, whole-mount immunostaining with α-HRP-Cy3 revealed that *AgAmtP*-driven *GFP* is expressed in both

Author Manuscript Author Manuscript Author Manuscript Author Manuscript

neuronal and auxiliary cells in the larval antennae (Figure 14A–14D). The *AgAmtP*-driven *GFP* expressing auxiliary cells surround, or are proximate to, most if not all of the α-HRP labelled neurons, which is consistent with a previous description of larval auxiliary cells (Figure 14A–14D) (Zacharuk et al., 1971). As expected, α-Orco polyclonal antibodies marked ORNs comprise a subset of these larval neurons (Figure 14B, 14F) and a close association between ORNs and what are likely to be *AgAmt*-expressing larval auxiliary cells was observed (Figure 14E–14H).

4. Discussion

4.1 Heterogeneous localization of *AgAmt* in Olfactory and Gustatory Appendages

From a technical perspective, the generation of a set of *AgAmtP-QF2* driver lines involved the development of a high-efficiency adaptation that brings together the phiC31 integration (Meredith et al., 2011) and Q system (Riabinina et al., 2016) in the malaria vector *An. gambiae* which until recently has been largely refractory to such genetic manipulations. We have utilized the phiC31 site-specific integration system to generate a Q system driver line thereby avoiding positional effects and potential fitness costs introduced by random-insertion transposon systems (Labbé et al., 2010). Additionally, the large integration capacity of the phiC31 system ensures the practicability of generating driver lines with larger transcriptional regulatory elements (Nimmo et al., 2006). Indeed, the relatively high integration efficiency of driver constructs we observed in *An. gambiae* is likely due to the use of the phiC31 helper plasmid as the source of integrase, as the plasmid is likely to be more stable and therefore better able to express integrase activity than co-injected mRNA (Gratz et al., 2014; Kistler et al., 2015). In this manner, we have developed a technical workflow where the driver line, and potentially, a modified effector line can be rapidly generated in *An. gambiae*. These substantial improvements in utility result in a highly efficient Q system that represents a powerful tool for the genetic characterization and manipulation of *An. gambiae* target genes in future studies.

In order to further characterize the role of *AgAmt* insofar as ammonia sensitivity and metabolic processes that are salient for host-seeking and other mosquito behaviors, we examined the spatial localization in the chemosensory appendages of the adult and larval peripheral nervous system of *An. gambiae*. Previous studies examining the localization of *DmAmt*, the *Amt* homolog in the chemosensory appendages of *D. melanogaster*, revealed an unexpected heterogeneity in which *DmAmt* is found in nonneuronal antennal auxiliary cells whereas in the labella and tarsi, *DmAmt* is neuronal (Delventhal et al., 2017; Menuz et al., 2014). Importantly, these *Drosophila* studies also revealed *DmAmt*'s functional heterogeneity; in which antennal expression is required for olfactory responses to ammonia, while null mutants which showed no labellum-expression also displayed wild-type gustatory responses to ammonium solutions (Delventhal et al., 2017; Menuz et al., 2014).

While acknowledging the reliance on *AgAmtP*-driven GFP signals, our localization studies in female *An. gambiae* antennae build upon the theme of heterogeneity by demonstrating that *AgAmtP*-derived *GFP* is widely expressed in both neuronal and non-neuronal cells (Figures 2–5). More specifically, and in contrast to *DmAmt* which is expressed only in a narrow subtype of antennal coeloconic sensilla (ac1) (Menuz et al., 2014), *AgAmtP*-driven

Author Manuscript Author Manuscript Author Manuscript Author Manuscript

GFP is expressed in the auxiliary cells in all coeloconic sensilla as well as what appears to be the majority of grooved pegs. Even more complexity is evident as neuronal *AgAmtP*-derived *GFP* expression seems to be localized to non-OSNs as these cells are not labelled by either α-Orco antibodies or *Ir76b* riboprobes. As is the case in *Drosophila* antennae (Menuz et al., 2014), we did not observe *AgAmtP*-derived *GFP* expression in any trichoid sensilla despite studies demonstrating ammonia sensitivity across these sensilla (Qiu et al., 2006). Therefore the significant diversity we observed in *AgAmtP*-driven *GFP* expression presumably correlates with heterogenous function along the antennae of *An. gambiae*.

The chemosensory ultrastructure of the *An. gambiae* maxillary palps has long been thought to contain a single, homogeneous class of olfactory sensilla, the capitate pegs, in which 3 distinct neurons are present: two ORNs and one CO_2 sensing gustatory receptor neuron (GRN) (Lu et al., 2007). However, our expression data challenges this model as in contrast to the antennae, where *AgAmt* appears to be expressed in auxiliary cells and non-ORN neurons, *AgAmt*-driven *GFP* is expressed only in a subset of the maxillary palp ORNs. This suggests there is a previously undescribed heterogeneity among the maxillary palp capitate peg ORNs of *An. gambiae* that may impact functionality and sensitivity to ammonia and perhaps other stimuli on this important chemosensory appendage.

In the proboscis and tarsi that encompass the adult gustatory appendages, the complete spectrum of labial chemosensory neurons (ORNs, IRNs, and GRNs) appear to express *AgAmt*. Moreover, all segments in the tarsi display *AgAmtP*-driven *GFP* expression compared to only up to 4 *DmAmt*$^+$ segments in *Drosophila* (Delventhal et al., 2017). Consistent with studies showing that *DmAmt* is expressed in the sugar sensing *DmGr5a* neurons instead of the ammonium sensing *DmGr66a* neurons (Delventhal et al., 2017), *AgAmtP*-driven *GFP* is expressed in the putative mosquito sugar sensing *AgGr15* neurons in the labellum. Inasmuch as mosquito tarsi have not been shown to display ammonia sensitivity, these data raise the possibility that the function of neuronal AgAmt is fundamentally different from the auxiliary cell AgAmt and indeed may not be directly involved in environmental ammonium sensing.

The *An. gambiae* larval antennae is a single tubular appendage in which the primary olfactory structure, the sensory cone, is located at the distal tip and is innervated by a group of subtended chemosensory neurons that are enveloped by auxiliary cells (Xia et al., 2008; Zacharuk et al., 1971). Although studies have revealed the potential olfactory function of the sensory cone (Xia et al., 2008), no electrophysiological studies have thus far been conducted to characterize the chemosensory responses of neurons in the larval antennae (Liu et al., 2010; Xia et al., 2008). Given that *AgAmtP*-driven GFP is localized in auxiliary cells surrounding a group of α-HRP labelled neurons among which ORNs only compose a subset, our data suggests that in larvae, AgAmt functionality is associated with other chemosensory neurons besides ORNs. Therefore, given the strong correlation between *Ag/DmAmt* expression and ammonia sensitivity that we and others have demonstrated (Delventhal et al., 2017; Menuz et al., 2014), it is reasonable to speculate that other structures/chemosensory neurons on the larval antennae, along with the ORN-innervated sensory cone (Xia et al., 2008), are involved in chemosensory processing of ammonia-based stimuli (Zacharuk and Blue, 1971).

Author Manuscript Author Manuscript Author Manuscript Author Manuscript

In addition to the expression of *AgOrco* and *AgOR*s that define ORNs, *AgIR* expression has been reported in larval IRNs and shown to mediate larvae behaviors (Liu et al., 2010). In light of previous studies in the larval antennae where ORNs seem to be exclusively present in the sensory cone (Xia et al., 2008) and in the adult chemosensory system that suggest IRNs and ORNs are distinct cell populations (Pitts et al., 2017) it is reasonable to speculate that larval *AgIRs* are expressed in chemosensory appendages other than the ORN-rich sensory cone that may correlate to larval ammonia sensitivity.

4.2 A Model for Neuronal Amt function

While it has been suggested that *DmAmt* expression in *Drosophila* antennal auxiliary cells is involved in ammonium clearance from the sensillar lymph to ameliorate receptor desensitization (Menuz et al., 2014), the function of neuronal *DmAmt* on the labellum remains cryptic (Delventhal et al., 2017). In contrast, apart from our observation of non-neuronal *AgAmtP*-driven *GFP* expression in antennal coeloconic and basiconic auxillary cells, *AgAmt* is largely neuronal across all the chemosensory appendages of *An. gambiae*. This begs the general question as to the function of neuronal ammonium transporters in the malaria mosquito.

It is reasonable to suggest that insect chemosensory neurons must transport ammonium for a variety of metabolic and/or neurobiological purposes that could be addressed by bidirectional *Amt* transporters (Durant and Donini, 2018; Soupene et al., 2002). Indeed, in honeybees it has been observed that ammonium is produced in the conversion of glutamine to glutamate in glutamatergic neurons and is released from photoreceptor neurons and transported to glial cells (Marcaggi and Coles, 2001; Tsacopoulos et al., 1997), where neuronal expressing *Amt* may be involved. While the ammonium excretion from neurons remains largely uncharacterized, it was suggested that the Na^+-K^+−$2Cl^-$ co-transporter plays a role in transporting ammonia into the honeybee glial cells by substituting the K^+ with ammonium (Bak et al., 2006; Marcaggi and Coles, 2001). However, this co-transporter has a moderate affinity for ammonium and is therefore less efficient in its transport (Bakouh et al., 2006). It is therefore possible that Amt is acting as a potential supporting element in this process. While glutamatergic interneurons have been characterized in the antennal lobes of *Drosophila*, no glutamatergic OSNs have been described in other insects. In addition to glutamate, gamma-aminobutyric acid (GABA) has also been shown to serve as an inhibitory neurotransmitter in insects (Wilson and Laurent, 2005). The GABAergic neurons requires a similar ammonia clearance system as the glutamatergic neurons where Amt can also be functional (Bak et al., 2006). While many studies suggest a large portion of glutamatergic/GABAergic cells act as local interneurons (LNs) concentrated in the insect antennal lobes, antennal GABAergic neurons have also been identified in the sphinx moth (Hoskins et al., 1986). Additionally, it is possible that neuronal Amt plays a role in the metabolism of biogenic amines which modulate neuronal activity (Zhukovskaya and Polyanovsky, 2017). Moreover, serotoninergic neurons were found in olfactory and gustatory appendages in mosquitoes (Siju et al., 2008; Zhukovskaya and Polyanovsky, 2017), where the uptake/excretion of ammonia could be essential for the regulation of serotonin synthesis (Coleman and Neckameyer, 2005; Grippon et al., 1986). While the function of DmAmt in gustatory appendages remains unknown, the high labial expression level of *Amt* in *Drosophila*,

Author Manuscript Author Manuscript Author Manuscript Author Manuscript

Anopheles, and *Aedes* suggests that a significant role of ammonium transporters in gustation or in labial-based olfaction that has been shown to occur in *An. gambiae* (Kwon et al., 2006; Matthews et al., 2016; Menuz et al., 2014; Pitts et al., 2014; Saveer et al., 2018).

4.3 *IR*s are implicated in ammonia detection

While Anopheline *OR*s are widely expressed on antennae and have been shown to recognize diverse combinations of chemical stimuli, they are not expressed in the ammonia-sensitive grooved pegs (Carey et al., 2010; Pitts et al., 2004; Wang et al., 2010). The characterization of *Drosophila IRs* as amine and acid receptors revealed *DmIr92a* is co-expressed with *DmIr76b* and *DmIr25a* co-receptors that together are responsible for olfactory responses to ammonia in ac1 coeloconic sensilla (Ai et al., 2010; Benton et al., 2009; Min et al., 2013). Recently, several similar amine and acid-sensitive *An. gambiae IR*s have been characterized (Pitts et al., 2017) although in the absence of a clear *DmIr92*a homolog, the Anopheline ammonia receptor has not yet been identified.

We have found a strong association between *AgAmt* and ammonia sensing neurons. In addition to the grooved pegs as previously demonstrated (Qiu et al., 2006), all of the putative *AgAmt*-expressing sensilla on the antennae and maxillary palps showed neuronal responses to ammonia. Moreover, the localization of antennal *AgAmtP*-driven GFP is highly correlated with *AgIr76b*, which suggests that, in keeping with the data from *Drosophila* (Menuz et al., 2014), mosquito ammonia receptors are likely to be *IR*s. In light of the high correlation between the response spectrum of *DmIRs* and *AgIRs* and the odor response profiles of *An. gambiae* grooved pegs (Benton et al., 2009; Pitts et al., 2017; Qiu et al., 2006), which are orthologous to *Drosophila* coeloconic sensilla (Ray, 2015), it is reasonable to suggest these sensilla are innervated by IRNs instead of ORNs, and that *AgIRs* are ammonia sensing receptors in Anopheline grooved pegs.

It is noteworthy that we did not observe *AgAmtP*-driven *GFP* expression in the trichoid sensilla, a subpopulation of which has been shown to house ammonia sensitive neurons (Qiu et al., 2006). This suggests there are *AgAmt*-independent ammonia sensing pathways in *An. gambiae*. Furthermore, inasmuch as *An. gambiae* trichoid sensilla express *Orco* and presumably a range of tuning *OR*s, it is likely this alternative pathway is *OR*-mediated and perhaps involves the antennal-expressed *Rh50* transporter (Pitts et al., 2014).

Supplementary Material

Refer to Web version on PubMed Central for supplementary material.

Acknowledgements

We thank Zhen Li for mosquito rearing, Dr. Ahmed Saveer (North Carolina State University) and Dr. Zhiwei Zhang (Shanxi Agricultural University) for technical training, and all members of the Zwiebel lab for valuable advice and comments throughout the course of this work. We also thank Dr. Julian Hillyer, Dr. Maulik Patel, Dr. Wenbiao Chen, and Dr. Patrick Abbot (Vanderbilt University) for critical suggestions. We are especially grateful for the generous gift of expertise and Q system mosquito lines from Dr. Christopher Potter (the Johns Hopkins University School of Medicine). Lastly, we acknowledge The Vanderbilt University Cell Imaging Shared Resource Core for training and use of the Olympus FV-1000 confocal microscope and Dr. James Patton (Vanderbilt University) for cryostat access. This work was conducted with the support of Vanderbilt University and funded by the National Institutes of Health (NIAID, R21-113960) to LJZ.

Author Manuscript Author Manuscript Author Manuscript Author Manuscript

Abbreviations

AgAmt	*Anopheles gambiae* ammonium transporter
DmAmt	*Drosophila melanogaster* ammonium transporter
AgAmtP	AgAmt promoter
IR	ionotropic receptor
OR	odorant receptor
GR	gustatory receptor
ORN	odorant receptor neuron
IRN	ionotropic receptor neuron
OSN	olfactory sensory neuron

References

Ai M, Min S, Grosjean Y, Leblanc C, Bell R, Benton R, Suh GSB, 2010 Acid sensing by the *Drosophila* olfactory system. Nature 468, 691–695. 10.1038/nature09537 [PubMed: 21085119]

Alonso P, Noor AM, 2017 The global fight against malaria is at crossroads. Lancet 390, 2532–2534. 10.1016/S0140-6736(17)33080-5 [PubMed: 29195688]

Andrade SLA, Einsle O, 2007 The Amt/Mep/Rh family of ammonium transport proteins (Review). Mol. Membr. Biol 24, 357–365. 10.1080/09687680701388423 [PubMed: 17710640]

Bak LK, Schousboe A, Waagepetersen HS, 2006 The glutamate/GABA-glutamine cycle: Aspects of transport, neurotransmitter homeostasis and ammonia transfer. J. Neurochem 98, 641–653. 10.1111/j.1471-4159.2006.03913.x [PubMed: 16787421]

Bakouh N, Benjelloun F, Cherif-Zahar B, Planelles G, 2006 The challengeof understanding ammonium homeostasis and the role of the Rh glycoproteins. Transfus. Clin. Biol 13, 139–146. 10.1016/j.tracli.2006.02.008 [PubMed: 16564724]

Benton R, Vannice KS, Gomez-Diaz C, Vosshall LB, 2009 Variant Ionotropic Glutamate Receptors as Chemosensory Receptors in *Drosophila*. Cell 136, 149–162. 10.1016/j.cell.2008.12.001 [PubMed: 19135896]

Bittsánszky A, Pilinszky K, Gyulai G, Komives T, 2015 Overcoming ammonium toxicity. Plant Sci. 231, 184–190. 10.1016/j.plantsci.2014.12.005 [PubMed: 25576003]

Boverhof DR, Wiescinski CM, Botham P, Lees D, Debruyne E, Repetto-Larsay M, Ladics G, Hoban D, Gamer A, Remmele M, Wang-Fan W, Ullmann LG, Mehta J, Billington R, Woolhiser MR, 2008 Interlaboratory validation of 1% pluronic L92 surfactant as a suitable, aqueous vehicle for testing pesticide formulations using the murine local lymph node assay. Toxicol. Sci 105, 79–85. 10.1093/toxsci/kfn117 [PubMed: 18556666]

Carey AF, Wang G, Su CY, Zwiebel LJ, Carlson JR, 2010 Odorant reception in the malaria mosquito *Anopheles gambiae*. Nature 464, 66–71. 10.1038/nature08834 [PubMed: 20130575]

Chasiotis H, Ionescu A, Misyura L, Bui P, Fazio K, Wang J, Patrick M, Weihrauch D, Donini A, 2016 An animal homolog of plant Mep/Amt transporters promotes ammonia excretion by the anal papillae of the disease vector mosquito *Aedes aegypti*. J. Exp. Biol 219, 1346–1355. 10.1242/jeb.134494 [PubMed: 26944496]

Coleman CM, Neckameyer WS, 2005 Serotonin synthesis by two distinct enzymes in *Drosophila melanogaster*. Arch. Insect Biochem. Physiol 59, 12–31. 10.1002/arch.20050 [PubMed: 15822093]

Cox FE, 2010 History of the discovery of the malaria parasites and their vectors. Parasites and Vectors 3. 10.1186/1756-3305-3-5

Author Manuscript Author Manuscript Author Manuscript Author Manuscript

Crawford NM, Forde BG, 2002 Molecular and Developmental Biology of Inorganic Nitrogen Nutrition. Arab. B 1, e0011 10.1199/tab.0011

Delventhal R, Menuz K, Joseph R, Park J, Sun JS, Carlson JR, 2017 The taste response to ammonia in *Drosophila*. Sci. Rep. 7 10.1038/srep43754

Den Otter CJ, Behan M, Maes FW, 1980 Single cell responses in female Pieris brassicae (Lepidoptera: Pieridae) to plant volatiles and conspecific egg odours. J. Insect Physiol 26, 465–472. 10.1016/0022-1910(80)90117-1

Durant AC, Donini A, 2018 Ammonia excretion in an osmoregulatory syncytium is facilitated by AeAmt2, a novel ammonia transporter in Aedes aegypti larvae. Front. Physiol 9 10.3389/fphys.2018.00339

Ghaninia M, Ignell R, Hansson BS, 2007 Functional classification and central nervous projections of olfactory receptor neurons housed in antennal trichoid sensilla of female yellow fever mosquitoes, *Aedes aegypti*. Eur. J. Neurosci 26, 1611–1623. 10.1111/j.1460-9568.2007.05786.x [PubMed: 17880395]

Gratz SJ, Ukken FP, Rubinstein CD, Thiede G, Donohue LK, Cummings AM, Oconnor-Giles KM, 2014 Highly specific and efficient CRISPR/Cas9-catalyzed homology-directed repair in *Drosophila*. Genetics 196, 961–971. 10.1534/genetics.113.160713 [PubMed: 24478335]

Grippon P, le Poncin Lafitte M, Boschat M, Wang S, Faure G, Dutertre D, Opolon P, 1986 Evidence for the role of ammonia in the intracerebral transfer and metabolism of tryptophan. Hepatology 6, 682–686. 10.1002/hep.1840060424 [PubMed: 2426170]

Guidobaldi F, May-Concha IJ, Guerenstein PG, 2014 Morphology and physiology of the olfactory system of blood-feeding insects. J. Physiol. Paris 108, 96–111. 10.1016/j.jphysparis.2014.04.006 [PubMed: 24836537]

Hoskins SG, Homberg U, Kingan TG, Christensen TA, Hildebrand JG, 1986 Immunocytochemistry of GABA in the antennal lobes of the sphinx moth *Manduca sexta*. Cell Tissue Res. 244, 243–252. 10.1007/BF00219199 [PubMed: 3521878]

Jan LY, Jan YN, 1982 Antibodies to horseradish peroxidase as specific neuronal markers in *Drosophila* and in grasshopper embryos. Proc. Natl. Acad. Sci. U. S. A 79, 2700–2704. 10.1073/pnas.79.8.2700 [PubMed: 6806816]

Kistler KE, Vosshall LB, Matthews BJ, 2015 Genome engineering with CRISPR Cas9 in the mosquito Aedes aegypti. Cell Rep. 11, 51–60. 10.1016/j.celrep.2015.03.009 [PubMed: 25818303]

Kwon HW, Lu T, Rützler M, Zwiebel LJ, 2006 Olfactory response in a gustatory organ of the malaria vector mosquito *Anopheles gambiae*. Proc. Natl. Acad. Sci. U. S. A 103, 13526–13531. 10.1073/pnas.0601107103 [PubMed: 16938890]

Labbé GMC, Nimmo DD, Alphey L, 2010 Piggybac- and PhiC31-mediated genetic transformation of the Asian tiger mosquito, Aedes albopictus (Skuse). PLoS Negl. Trop. Dis 4 10.1371/journal.pntd.0000788

Leal WS, 2013 Odorant Reception in Insects: Roles of Receptors, Binding Proteins, and Degrading Enzymes. Annu. Rev. Entomol 58, 373–391. 10.1146/annurev-ento-120811-153635 [PubMed: 23020622]

Liu C, Pitts RJ, Bohbot JD, Jones PL, Wang G, Zwiebel LJ, 2010 Distinct olfactory signaling mechanisms in the malaria vector mosquito *Anopheles gambiae*. PLoS Biol. 8, 27–28. 10.1371/journal.pbio.1000467

Liu F, Chen L, Appel AG, Liu N, 2013 Olfactory responses of the antennal trichoid sensilla to chemical repellents in the mosquito, *Culex quinquefasciatus*. J. Insect Physiol 59, 1169–1177. 10.1016/j.jinsphys.2013.08.016 [PubMed: 24035746]

Loesel R, Weigel S, Bräunig P, 2006 A simple fluorescent double staining method for distinguishing neuronal from non-neuronal cells in the insect central nervous system. J. Neurosci. Methods 155, 202–206. 10.1016/j.jneumeth.2006.01.006 [PubMed: 16481042]

Lu T, Qiu YT, Wang G, Kwon JY, Rutzler M, Kwon HW, Pitts RJ, van Loon JJA, Takken W, Carlson JR, Zwiebel LJ, 2007 Odor coding in the maxillary palp of the malaria vector mosquito *Anopheles gambiae*. Curr. Biol 17, 1533–1544. 10.1016/j.cub.2007.07.062 [PubMed: 17764944]

Author Manuscript Author Manuscript Author Manuscript Author Manuscript

Marcaggi P, Coles JA, 2001 Ammonium in nervous tissue: Transport across cell membranes, fluxes from neurons to glial cells, and role in signalling. Prog. Neurobiol 64, 157–183. 10.1016/S0301-0082(00)00043-5 [PubMed: 11240211]

Matthews BJ, McBride CS, DeGennaro M, Despo O, Vosshall LB, 2016 The neurotranscriptome of the *Aedes aegypti* mosquito. BMC Genomics 17 10.1186/s12864-015-2239-0

McIver SB, 1973 Fine structure of antennal sensilla coeloconica of culicine mosquitoes. Tissue Cell 5, 105–112. 10.1016/S0040-8166(73)80009-6 [PubMed: 4693984]

Mclver SB, 1982 Sensilla of mosquitoes (Diptera: Culicidae)1, 2. J. Med. Entomol 19, 489–535. 10.1093/jmedent/19.5.489 [PubMed: 6128422]

Meijerink J, Braks MAH, Van Loon JJA, 2001 Olfactory receptors on the antennae of the malaria mosquito *Anopheles gambiae* are sensitive to ammonia and other sweat-borne components. J. Insect Physiol 47, 455–464. 10.1016/S0022-1910(00)00136-0 [PubMed: 11166310]

Menuz K, Larter NK, Park J, Carlson JR, 2014 An RNA-Seq screen of the *Drosophila* antenna identifies a transporter necessary for ammonia detection. PLoS Genet. 10 10.1371/journal.pgen.1004810

Meredith JM, Basu S, Nimmo DD, Larget-Thiery I, Warr EL, Underhill A, McArthur CC, Carter V, Hurd H, Bourgouin C, Eggleston P, 2011 Site-specific integration and expression of an anti-malarial gene in transgenic *Anopheles gambiae* significantly reduces *Plasmodium* infections. PLoS One 6 10.1371/journal.pone.0014587

Min S, Ai M, Shin SA, Suh GSB, 2013 Dedicated olfactory neurons mediating attraction behavior to ammonia and amines in *Drosophila*. Proc. Natl. Acad. Sci. U. S. A 110, 1321–1329. 10.1073/pnas.1215680110 [PubMed: 23297233]

Molina-Cruz A, Zilversmit MM, Neafsey DE, Hartl DL, Barillas-Mury C, 2016 Mosquito vectors and the globalization of *Plasmodium falciparum* malaria. Annu. Rev. Genet 50, 447–465. 10.1146/annurev-genet-120215-035211 [PubMed: 27732796]

Montell C, Zwiebel LJ, 2016 Mosquito sensory systems. Adv. In Insect Phys 51, 293–328. 10.1016/bs.aiip.2016.04.007

Mukabana WR, Mweresa CK, Otieno B, Omusula P, Smallegange RC, van Loon JJA, Takken W, 2012 A novel synthetic odorant blend for trapping of malaria and other African mosquito species. J. Chem. Ecol 38, 235–244. 10.1007/s10886-012-0088-8 [PubMed: 22426893]

Nimmo DD, Alphey L, Meredith JM, Eggleston P, 2006 High efficiency site-specific genetic engineering of the mosquito genome. Insect Mol. Biol 15, 129–136. 10.1111/j.1365-2583.2006.00615.x [PubMed: 16640723]

Pitts RJ, Derryberry SL, Pulous FE, Zwiebel LJ, 2014 Antennal-expressed ammonium transporters in the malaria vector mosquito *Anopheles gambiae*. PLoS One 9 10.1371/journal.pone.0111858

Pitts RJ, Derryberry SL, Zhang Z, Zwiebel LJ, 2017 Variant ionotropic receptors in the malaria vector mosquito *Anopheles gambiae* tuned to amines and carboxylic acids. Sci. Rep 7 10.1038/srep40297

Pitts RJ, Fox AN, Zwiebeil LJ, 2004 A highly conserved candidate chemoreceptor expressed in both olfactory and gustatory tissues in the malaria vector *Anopheles gambiae*. Proc. Natl. Acad. Sci. U. S. A 101, 5058–5063. 10.1073/pnas.0308146101 [PubMed: 15037749]

Pitts RJ, Zwiebel LJ, 2006 Antennal sensilla of two female anopheline sibling species with differing host ranges. Malar. J 5 10.1186/1475-2875-5-26

Pondeville E, Puchot N, Meredith JM, Lynd A, Vernick KD, Lycett GJ, Eggleston P, Bourgouin C, 2014 Efficient φc31 integrase-mediated site-specific germline transformation of *Anopheles gambiae*. Nat. Protoc 9, 1698–1712. 10.1038/nprot.2014.117 [PubMed: 24945385]

Potter CJ, Tasic B, Russler EV, Liang L, Luo L, 2010 The Q system: A repressible binary system for transgene expression, lineage tracing, and mosaic analysis. Cell 141, 536–548. 10.1016/j.cell.2010.02.025 [PubMed: 20434990]

Qiu YT, van Loon JJA, Takken W, Meijerink J, Smid HM, 2006 Olfactory coding in antennal neurons of the malaria mosquito, *Anopheles gambiae*. Chem. Senses 31, 845–863. 10.1093/chemse/bjl027 [PubMed: 16963500]

Ray A, 2015 Reception of odors and repellents in mosquitoes. Curr. Opin. Neurobiol 34, 158–164. 10.1016/j.conb.2015.06.014 [PubMed: 26202080]

Author Manuscript Author Manuscript Author Manuscript Author Manuscript

Report WM, 1980 World. Chem. Eng. News 58, 28 10.1016/S0264-410X(07)01183-8 [PubMed: 11663066]

Riabinina O, Task D, Marr E, Lin CC, Alford R, O'Brochta DA, Potter CJ, 2016 Organization of olfactory centres in the malaria mosquito *Anopheles gambiae*. Nat. Commun 7 10.1038/ncomms13010

Saveer AM, Pitts RJ, Ferguson ST, Zwiebel LJ, 2018 Characterization of chemosensory responses on the labellum of the malaria vector mosquito, Anopheles coluzzii. Sci. Rep 8 10.1038/s41598-018-23987-y

Shanbhag SR, Müller B, Steinbrecht RA, 2000 Atlas of olfactory organs of *Drosophila melanogaster* 2. Internal organization and cellular architecture of olfactory sensilla. Arthropod Struct. Dev 29, 211–229. 10.1016/S1467-8039(00)00028-1 [PubMed: 18088928]

Siju KP, Hansson BS, Ignell R, 2008 Immunocytochemical localization of serotonin in the central and peripheral chemosensory system of mosquitoes. Arthropod Struct. Dev 37, 248–259. 10.1016/j.asd.2007.12.001 [PubMed: 18424232]

Smallegange RC, Geier M, Takken W, 2002 Behavioural responses of *Anopheles gambiae* to ammonia, lactic acid and a fatty acid in a y-tube olfactometer. Proc. Exp. Appl. Entomol 13, 147–152.

Smallegange RC, Qiu YT, van Loon JA, Takken W, 2005 Synergism between ammonia, lactic acid and carboxylic acids as kairomones in the host-seeking behaviour of the malaria mosquito *Anopheles gambiae* sensu stricto (Diptera: Culicidae). Chem. Senses 30, 145–152. 10.1093/chemse/bji010 [PubMed: 15703334]

Soupene E, Lee H, Kustu S, 2002 Ammonium/methylammonium transport (Amt) proteins facilitate diffusion of NH3 bidirectionally. Proc. Natl. Acad. Sci. U. S. A 99, 3926–3931. 10.1073/pnas.062043799 [PubMed: 11891327]

Suh E, Bohbot JD, Zwiebel LJ, 2014 Peripheral olfactory signaling in insects. Curr. Opin. Insect Sci 6, 86–92. 10.1016/j.cois.2014.10.006 [PubMed: 25584200]

Trussell LO, Fischbach GD, 1989 Glutamate receptor desensitization and its role in synaptic transmission. Neuron 3, 209–218. 10.1016/0896-6273(89)90034-2 [PubMed: 2576213]

Tsacopoulos M, Poitry-Yamate CL, Poitry S, 1997 Ammonium and glutamate released by neurons are signals regulating the nutritive function of a glial cell. J. Neurosci 17, 2383–2390. 10.1523/jneurosci.17-07-02383.1997 [PubMed: 9065499]

Van Der Goes Van Naters W, Carlson JR, 2006 Insects as chemosensors of humans and crops. Nature 444, 302–307. 10.1038/nature05403 [PubMed: 17108954]

Wang G, Carey AF, Carlson JR, Zwiebel LJ, 2010 Molecular basis of odor coding in the malaria vector mosquito *Anopheles gambiae*. Proc. Natl. Acad. Sci. U. S. A 107, 4418–4423. 10.1073/pnas.0913392107 [PubMed: 20160092]

Wilson RI, Laurent G, 2005 Role of GABAergic inhibition in shaping odor-evoked spatiotemporal patterns in the *Drosophila* antennal lobe. J. Neurosci 25, 9069–9079. 10.1523/JNEUROSCI.2070-05.2005 [PubMed: 16207866]

Xia Y, Wang G, Buscariollo D, Pitts RJ, Wenger H, Zwiebel LJ, 2008 The molecular and cellular basis of olfactory-driven behavior in *Anopheles gambiae* larvae. Proc. Natl. Acad. Sci. U. S. A 105, 6433–6438. 10.1073/pnas.0801007105 [PubMed: 18427108]

Zacharuk RY, Blue SG, 1971 Ultrastructure of a chordotonal and a sinusoidal peg organ in the antenna of larval *Aedes* aegypti (L.). Can. J. Zool 49, 1223–1230. 10.1139/z71-185 [PubMed: 5092642]

Zacharuk RY, Yin LR, Blue SG, 1971 Fine structure of the antenna and its sensory cone in larvae of Aedes aegypti (L.). J. Morphol 135, 273–297. 10.1002/jmor.1051350303 [PubMed: 5126255]

Zhukovskaya MI, Polyanovsky AD, 2017 Biogenic amines in insect antennae. Front. Syst. Neurosci 11 10.3389/fnsys.2017.00045

Zwiebel LJ, Takken W, 2004 Olfactory regulation of mosquito-host interactions. Insect Biochem. Mol. Biol 34, 645–652. 10.1016/j.ibmb.2004.03.017 [PubMed: 15242705]

Author Manuscript Author Manuscript Author Manuscript Author Manuscript

Highlights

- Comprehensive cellular localization of *AgAmt* in primary and accessory chemosensory appendages of mosquitoes using transgenic Q system;
- Heterogeneous expression pattern of *AgAmt* in both neuronal and non-neuronal cells;
- Significant ammonia sensitivity in *AgAmt*-expressing sensilla.

Author Manuscript Author Manuscript Author Manuscript Author Manuscript

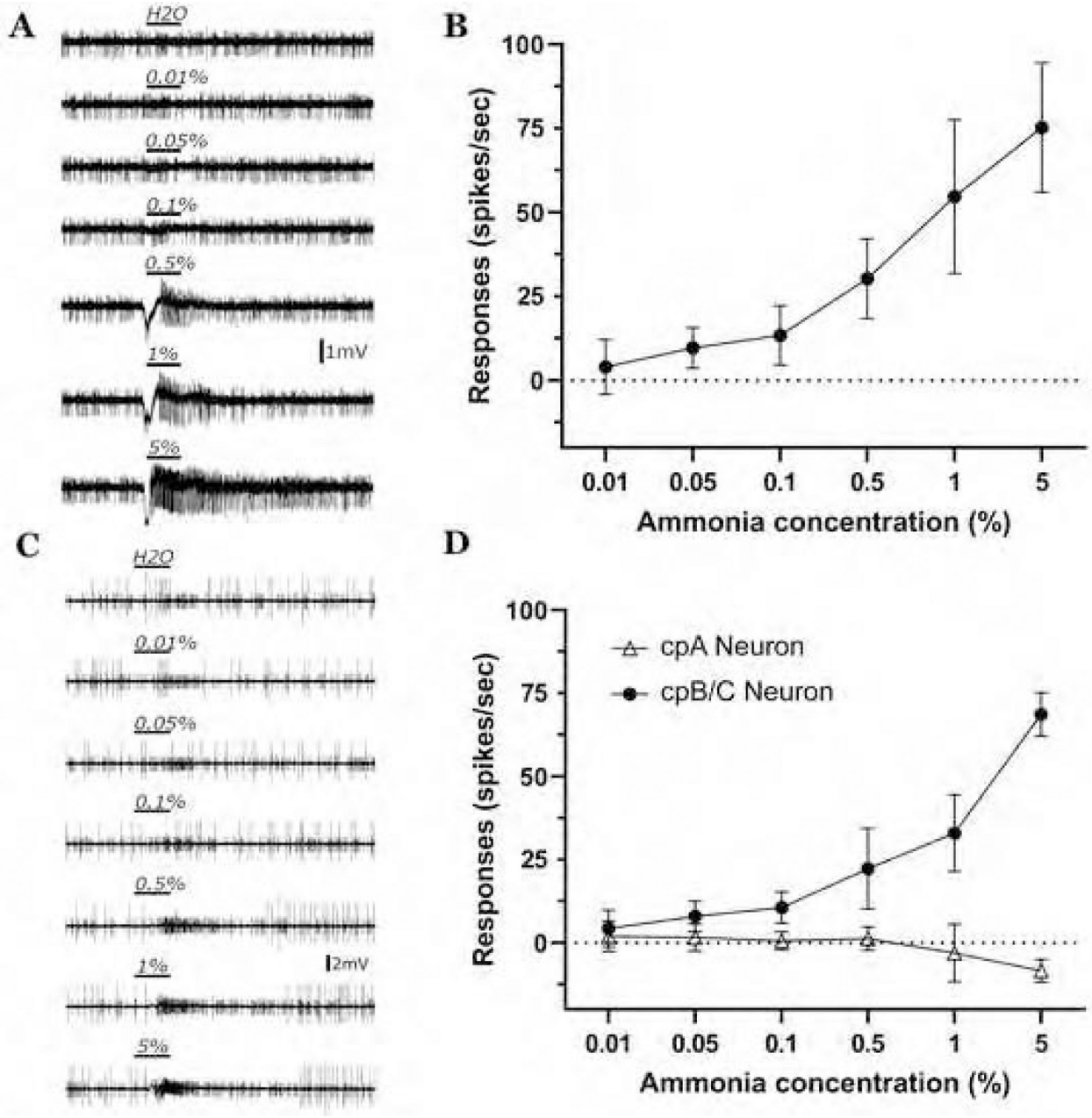

Figure 1.

Schematics of PCR strategies to validate: **(A)** the phiC31 site specific integration using two primer pairs that cover the integration junctions; **(B)** the unintegrated attP attachment site; **(C)** the *1kb AgAmtP* using a primer pair that spans the *1kb promoter-QF* sequences; **(D)** the *3kb AgAmtP* using a primer pair that spans the *3kb promoter-QF* sequences. **(E-G)** The gel image of the PCR validation on 1kb drivers **(E)**, 3kb drivers **(F)**, and docking lines **(G)**. For each mosquito line, the lanes from left to right are using primer pairs: attR_F/attR_R (**AR**, 224bp), attL_F/attL_R (**AL**, 301 bp), attP_F/attP_R (**B**, 391bp), 1kb_F/QF_R (**C**, 792bp), and 3kb_F/QF_R (**D**, 1.7kb), respectively.

Author Manuscript Author Manuscript Author Manuscript Author Manuscript

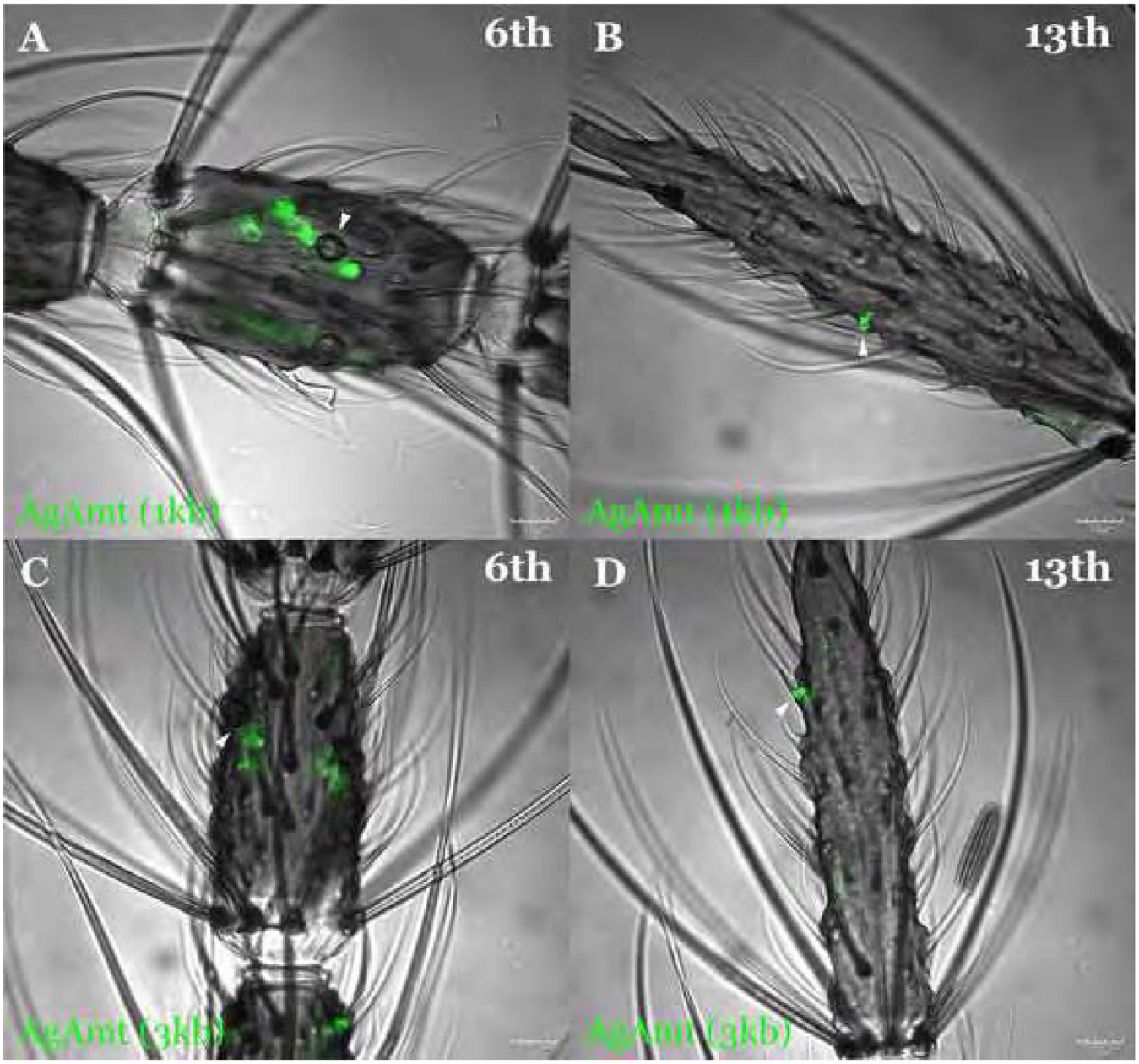

Figure 2.

The confocal optical section of the whole-mount female *An. gambiae* antennae carrying *QUAS-GFP* and either *1kb AgAmtP-QF2* (**A, B**; green) or *3kb AgAmtP-QF2* (**C, D**; green) constructs showing specific expression of *GFP* in coeloconic sensilla on the 6th flagellomere (**A, C**) and grooved pegs on the 13th flagellomere (**B, D**). Sensilla are highlighted with white arrows. Scale bars = 10μm.

Author Manuscript Author Manuscript Author Manuscript Author Manuscript

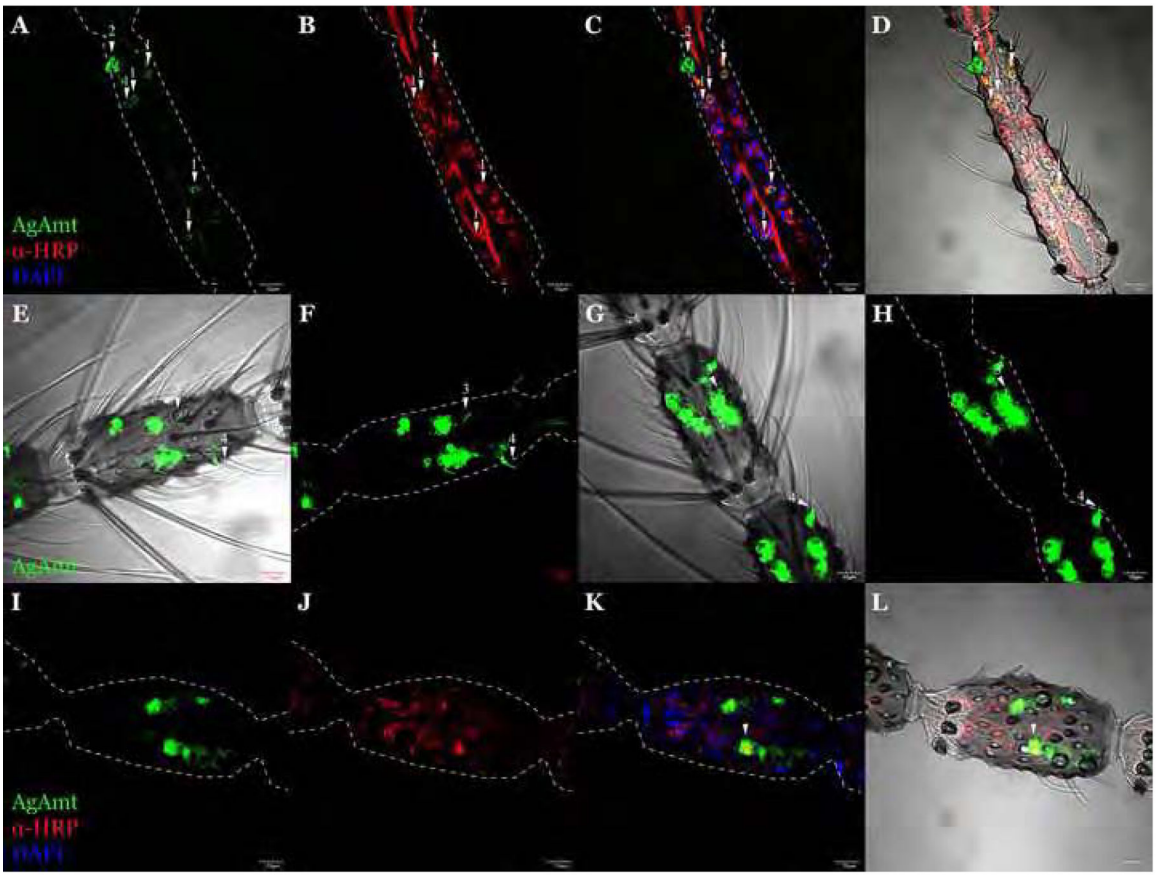

Figure 3.

The confocal optical section of immunohistochemistry staining on the female antennae using α-HRP (red) showing *AgAmtP*-driven *GFP* (green) is expressed in both neuronal (arrow 1) and non-neuronal cells (arrow 2) (**A-D**). Z-axis projection of the whole-mount antennal female *An. gambiae* 6th flagellomere showing *AgAmt* dendritic labelling in coeloconic sensilla (arrow 3) and grooved pegs (arrow 4) of 1kb *AgAmtPGFP* progeny (**E, F**) and 3kb *AgAmtP-GFP* progeny (**G, H**). The confocal optical section showing a partial overlapping between GFP and α-HRP labeled cells (**I-L**). Scale bars = 10μm.

Author Manuscript Author Manuscript Author Manuscript Author Manuscript

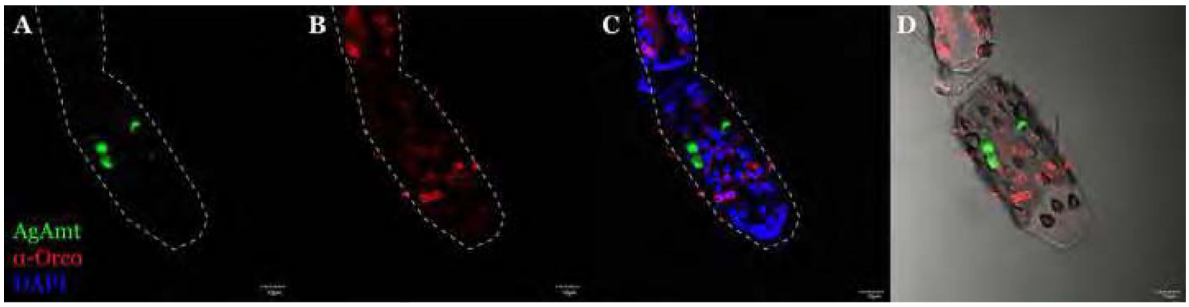

Figure 4.

A representative confocal optical section from adult *An. gambiae* female antennae immunohistochemically stained using α-Orco antibodies (red) showing that *AgAmtP*-driven *GFP* (green) and *Orco* are expressed in distinct cells (**A**-**D**). Scale bars = 10μm.

Author Manuscript Author Manuscript Author Manuscript Author Manuscript

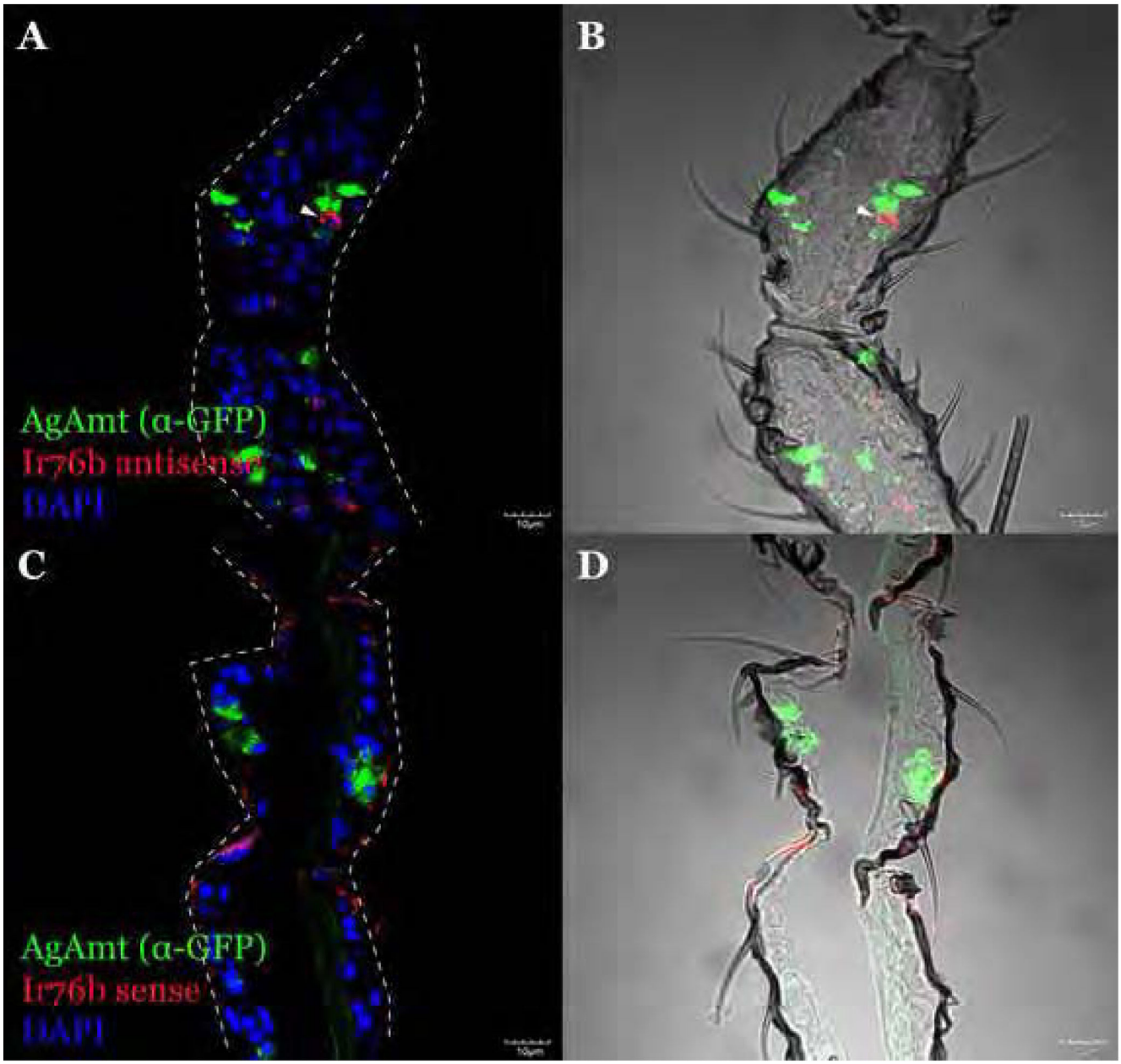

Figure 5.

A representative confocal optical section of FISH on the female antennae using *Ir76b* antisense riboprobe (red) and α-GFP showing *AgAmtP*-driven *GFP* (green) is expressed in auxiliary cells closely associated with *Ir76b*-expressing neurons (**A, B**). *Ir76b* sense riboprobe was used as the negative control for riboprobe specificity (**C, D**). An *Ir76b*-expressing cell is highlighted by arrows. Scale bars = 10μm.

Author Manuscript Author Manuscript Author Manuscript Author Manuscript

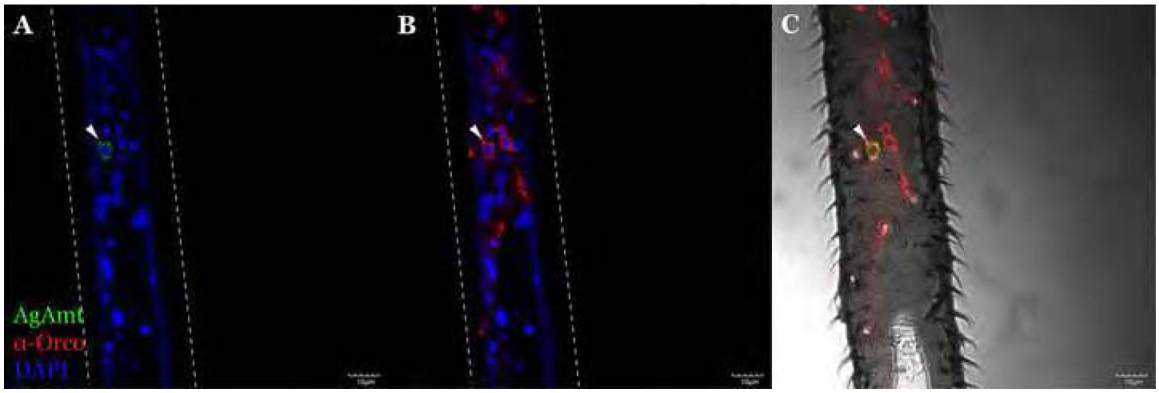

Figure 6.

A representative confocal optical section of adult female *An. gambiae* maxillary palps immunohistochemically stained with α-Orco antibodies (red) showing co-localization of *AgAmtP*-driven GFP (green) and Orco. An *AgAmtP*-derived *GFP* and *Orco* co-expressing cell is highlighted by arrows. Scale bars = 10μm.

Author Manuscript Author Manuscript Author Manuscript Author Manuscript

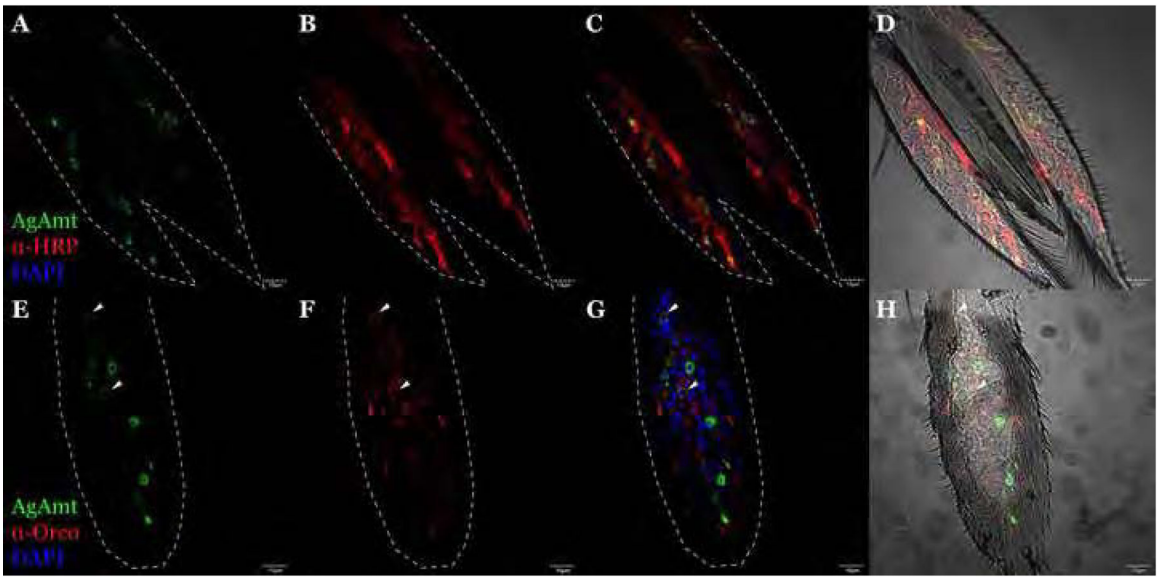

Figure 7. (A)

Single sensillum recording signals from a coeloconic sensillum to different concentrations of ammonia and the solvent. The vertical bar denotes the amplitude and the horizontal bar denotes the 0.5s duration of chemical stimulation; **(B)** Mean dose-dependent single sensillum responding patterns of coeloconic sensilla to six concentrations of ammonia; **(C)** Single sensillum recording signals from a capitate peg to different concentrations of ammonia and the solvent. The vertical bar denotes the amplitude and the horizontal bar denotes the 0.5s duration of chemical stimulation; **(D)** Mean dose-dependent single sensillum responding patterns of cpA neurons and cpB/C neurons in capitate pegs to six concentrations of ammonia. Error bars = Standard error of the mean.

Author Manuscript Author Manuscript Author Manuscript Author Manuscript

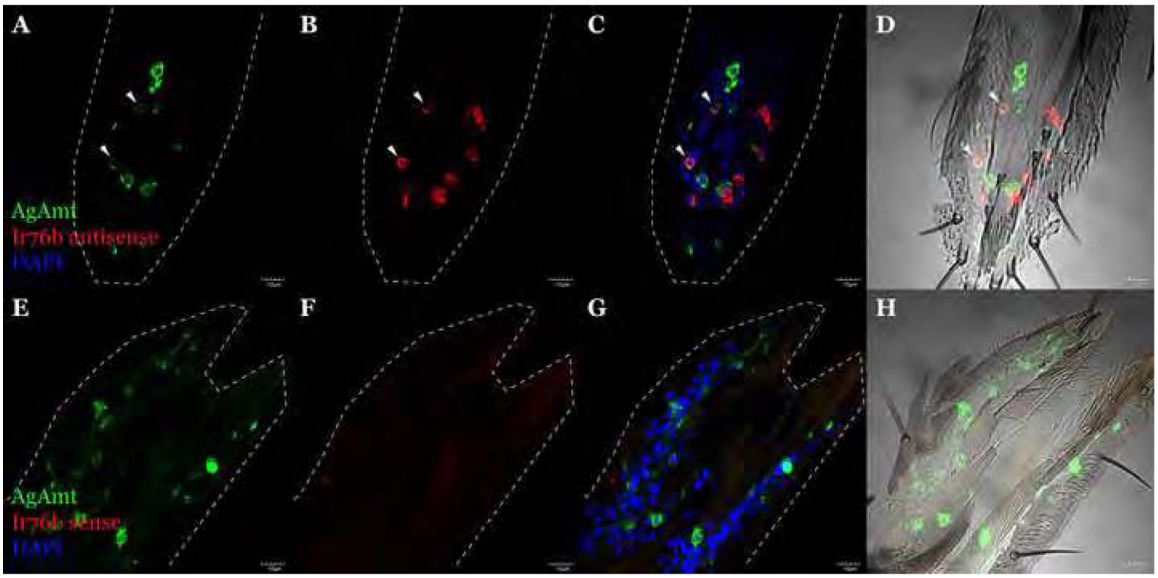

Figure 8.

Z-axis projection of whole-mount adult female *An. gambiae* labellum carrying *QUAS-GFP* and either *1kb AgAmtP-QF2* (**A-B**) or *3kb AgAmtP-QF2* (**C-D**) constructs showing specific expression of *GFP*. Dendritic labelling of *AgAmt* in T1 sensilla is highlighted by arrows. Scale bars = 10μm.

Author Manuscript Author Manuscript Author Manuscript Author Manuscript

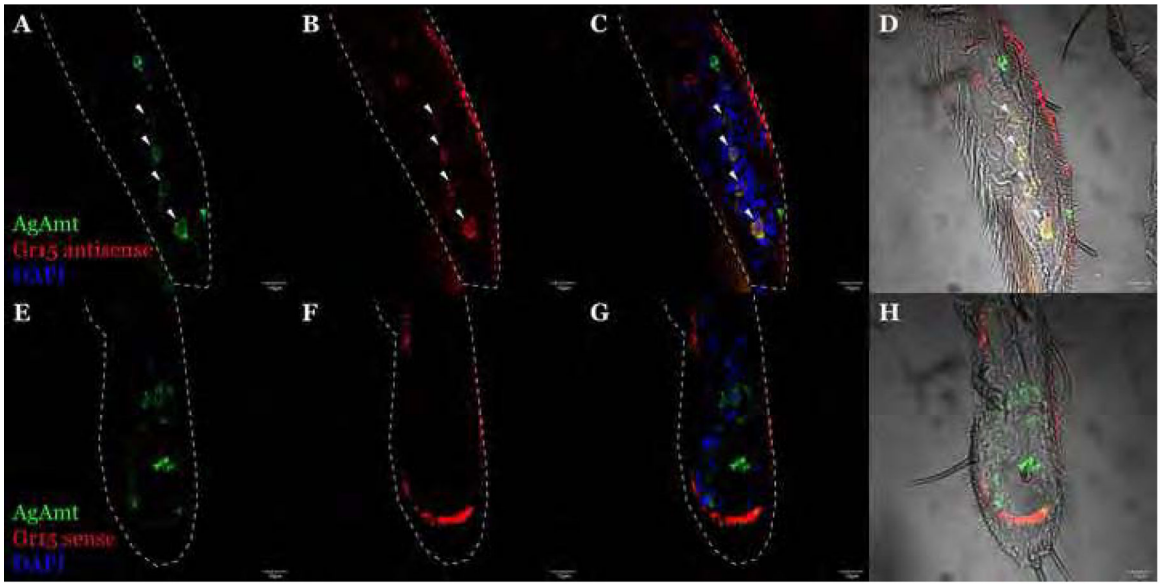

Figure 9.

A representative confocal optical section of adult female labellum immunohistochemically stained with α-HRP **(A-D**; red) and α-Orco **(E-H**; red) showing *AgAmtP*-driven *GFP* (green) is expressed in neurons and partially in ORNs. *AgAmtP*-derived *GFP* and *Orco* co-expressing cells are highlighted by arrows. Scale bars = 10μm.

Author Manuscript Author Manuscript Author Manuscript Author Manuscript

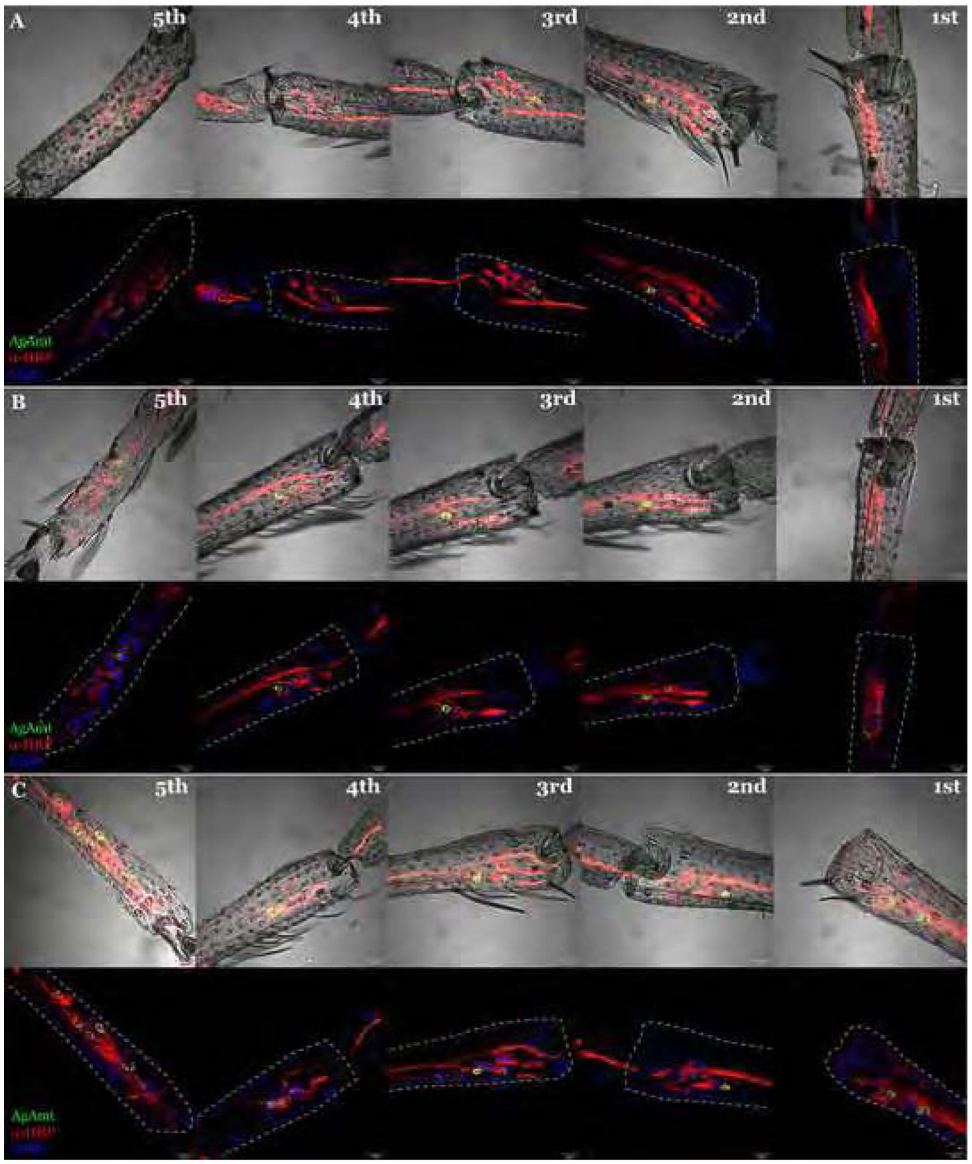

Figure 10.

A representative confocal optical section of the adult female labellum stained for FISH using *Ir76b* antisense riboprobes (red) and α-GFP showing partial *AgAmtP*-derived *GFP* (green) expression in *Ir76b*-expressing neurons (**A-D**). *Ir76b* sense riboprobes were used as the negative control for riboprobe specificity (**E-H**). *AgAmtP*- derived *GFP* and *Ir76b* co-expressing cells are highlighted by arrows. Scale bars = 10μm.

Author Manuscript
Author Manuscript
Author Manuscript
Author Manuscript

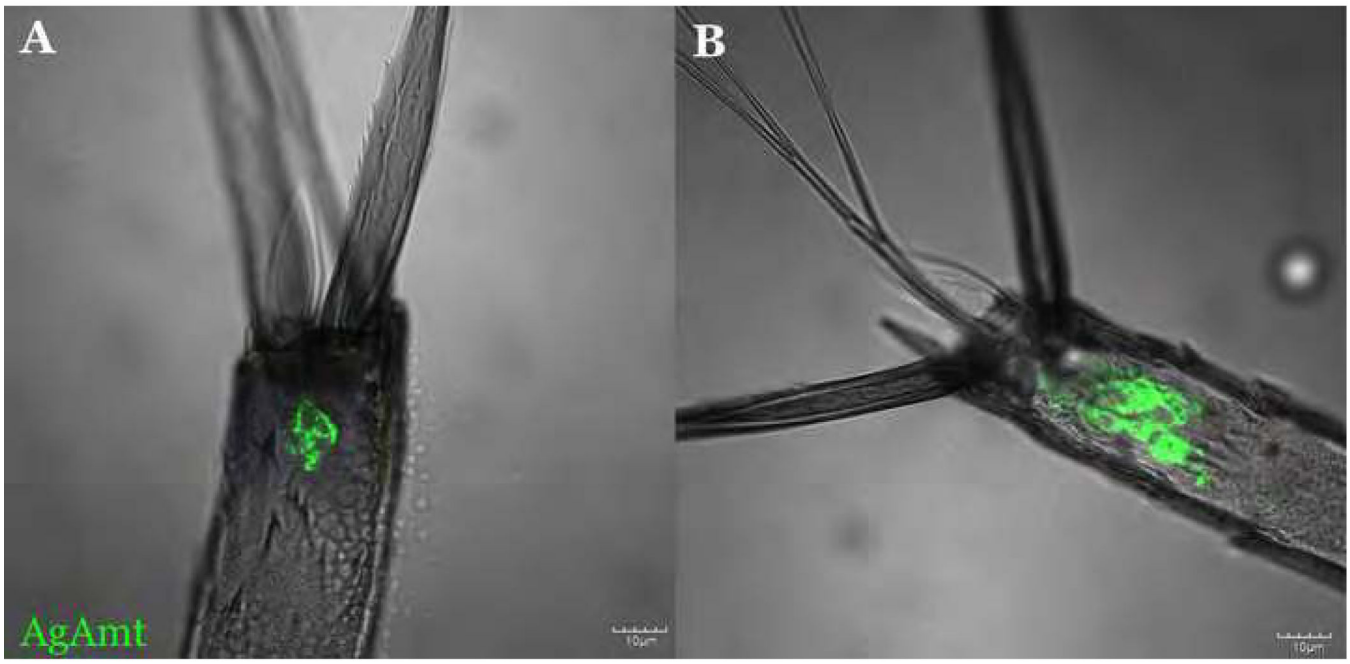

Figure 11.

A representative confocal optical section of the adult female labellum stained for FISH using *Gr15* antisense riboprobes (red) and α-GFP (green) showing partial *AgAmtP*-derived *GFP* expression in the *Gr15*-expressing neurons (**A-D**). *Gr15* sense riboprobes were used as the negative control for riboprobe specificity (**E-H**). *AgAmtP*-driven *GFP* and *Gr15* co-expressing cells are highlighted by arrows. Scale bars = 10μm.

Author Manuscript Author Manuscript Author Manuscript Author Manuscript

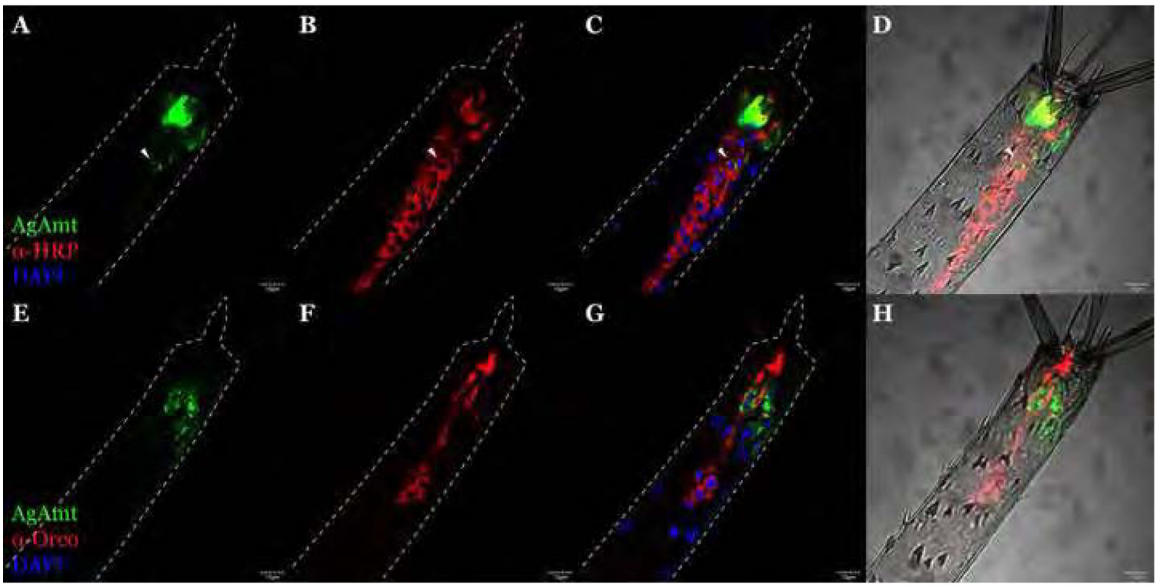

Figure 12.

A representative confocal optical section of adult female tarsi immunohistochemically stained with α-HRP (red) showing *AgAmtP-GFP* (green) is expressed in neurons in all five segments (1st-5th labelled on images) of protarsi **(A)**, mesotarsi **(B)**, and metatarsi **(C)**. Scale bars = 10μm.

Author Manuscript Author Manuscript Author Manuscript Author Manuscript

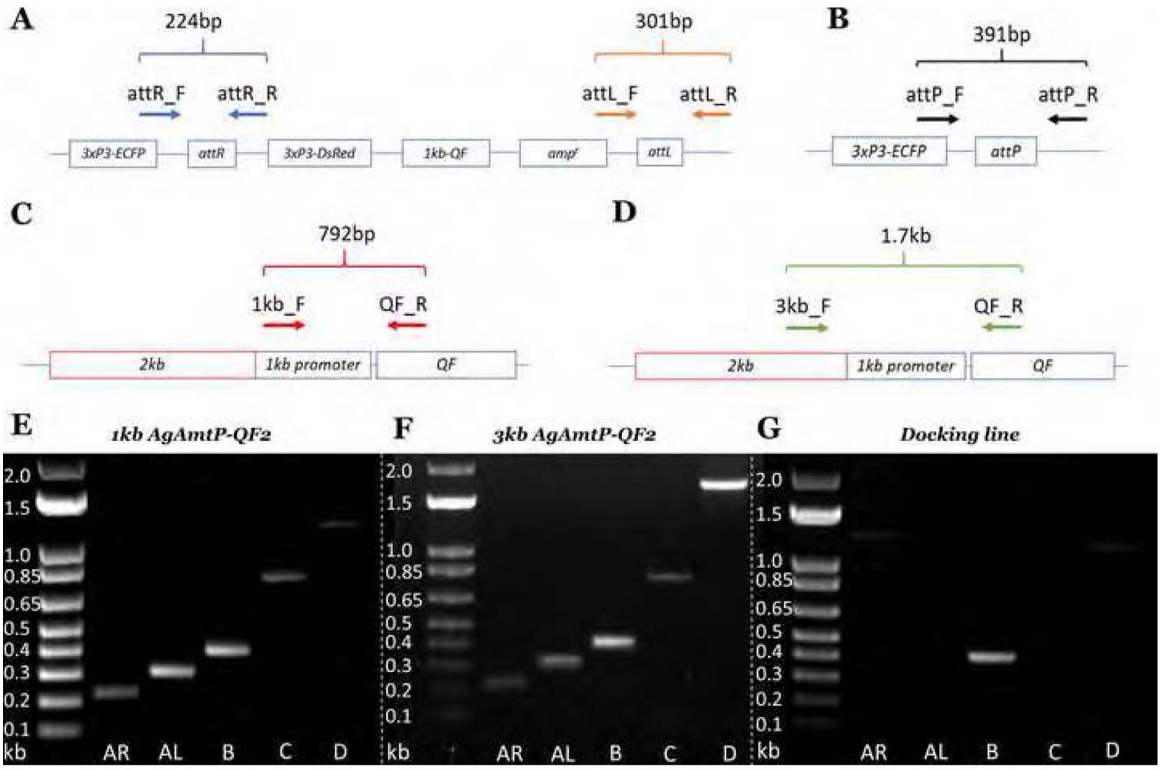

Figure 13.

A representative confocal optical section of whole-mount *An. gambiae* larval antennae carrying either *1kb* **(A)** or *3kb* **(B)** *AgAmtP-QF2* and *QUAS-GFP* showing *AgAmtP-GFP* (green) expression closely associated with the antennal sensory cone. Scale bars = 10μm.

Author Manuscript Author Manuscript Author Manuscript Author Manuscript

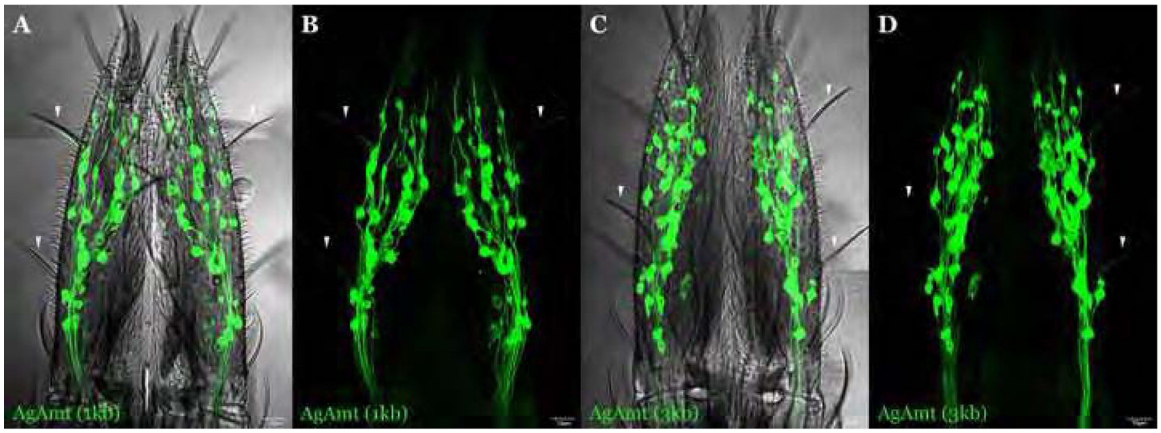

Figure 14.

A representative confocal optical section of whole-mount *An. gambiae* larval antennae from 3kb *AgAmtP-GFP* (green) progeny immunohistochemically stained with α-HRP **(A-D**; red) and α-Orco **(E-H**; red(showing *AgAmtP*-driven *GFP* expression in both neuronal cells and auxiliary cells which envelope the neurons. An *AgAmtP-GFP*-expressing neuron is highlighted by arrows. Scale bars = 10μm.

Author Manuscript

Author Manuscript

Author Manuscript

Author Manuscript

Table 1.

Details of embryo microinjection and the efficiency of phiC31 integration. The survived adults were pooled and crossed to the docking line opposite gender mosquitoes, and therefore the number of founders is the minimum.

Injected construct	Injected embryos	Survived adults	Founders
pBattB-DsRed-1 kb	1176	14 males	≥ 7.4% (2/27)
AgAmtP-QF2		13 females	
pBattB-DsRed-3kb	572	5 females	≥ 20% (1/5)
AgAmtP-QF2			